Development of High-Power Pulsed Fibre Laser Using Master Oscillator Power Amplifier (MOPA) System

Nathaniel Leong Jenn Kwang

A project report submitted in partial fulfilment of the requirements for the award of Bachelor of Science (Honours) Physics

Lee Kong Chian Faculty of Engineering and Science
Universiti Tunku Abdul Rahman

May 2020

DECLARATION

I hereby declare that this project report is based on my original work except for citations and quotations which have been duly acknowledged. I also declare that it has not been previously and concurrently submitted for any other degree or award at UTAR or other institutions.

Signature : _____

Name : Nathaniel Leong Jenn Kwang

ID No. : 1705711

Date : 14/9/2020

APPROVAL FOR SUBMISSION

I certify that this project report entitled **Development of High-Power PulsedFibre Laser Using Master Oscillator Power Amplifier (MOPA) System** was prepared by **Nathaniel Leong Jenn Kwang** has met the required standard for submission in partial fulfilment of the requirements for the award of Bachelor of Science (Honours) Physics at Universiti Tunku Abdul Rahman.

Approved by,

Signature :

Supervisor : Dr. Pua Chang Hong

Date : 28/09/2020

Signature :

Co-Supervisor :

Date :

The copyright of this report belongs to the author under the terms of the copyright Act 1987 as qualified by Intellectual Property Policy of Universiti Tunku Abdul Rahman. Due acknowledgement shall always be made of the use of any material contained in, or derived from, this report.

ACKNOWLEDGEMENTS

I would like to thank my supervisor, Dr. Pua Chang Hong for his guidance and advice during the course of this research. I would also like to thank him for assisting me with liasing with Photonics Research Centre, University Malaya for this research.

Special thanks to Dr. Chong Wu Yi for the opportunity to work in Photonics Research Centre, Universiti Malaya. I would like to extend my appreciation to Ng Kok Bin for his help and assistance when I'm carrying out my research. His help has been invaluable for my work. I am very grateful for his guidance throughout this research.

ABSTRACT

Mode-locked lasers are lasers with ultrashort pulses, typically in the range of a few femtoseconds. The mode-locked laser has many applications such as z-scan to determine non-linear index of a material and micromachining of transparent material. However, conventional solid state mode-locked lasers are large and expensive and require a complicated cooling system. A mode-locked fibre laser is inexpensive and is less bulky. However, they are not able to produce high output power that is comparable to the conventional solid state mode-locked laser. Therefore, to obtain high power, amplification is required. In this research, a mode-locked fibre laser using graphene oxide (GO) as saturable absorber will be developed. The mode-locked pulses will then be amplified using a two-stage amplification process to obtain higher output power. Due to non-linear effects in the fibre, the pulse will be significantly broadened due to supercontinuum generation which will be minimised by adding a length of single mode fibre (SMF) to broaden the pulse before amplification to reduce the intensity and thus, reduce the non-linear effects. This system is able to produce output power up to 164 mW. Some recommendations to further increase the output power and improve the performance of the mode-locked fibre laser system are given in this report.

TABLE OF CONTENTS

LIST OF TABLES

LIST OF FIGURES

LIST OF SYMBOLS / ABBREVIATIONS

c	Speed of light in vacuum
$\Delta\tau$	Pulse width broadenning
Δv	Spectral broadening in terms of frequency
$\Delta\lambda$	Spectral broadening in terms of wavelength
45TFG	45° tilted fibre grating
DMF	Dimethylformamide
EDF	Erbium-doped fibre
EDFA	Erbium-doped fibre amplifier
FC/APC	Fibre connector/angled physical contact
GO	Graphene oxide
MoS_2	Molybdenum disulphide
NALM	Non-linear amplifying loop mirror
OSA	Optical spectrum analyser
OC	Output coupler
PBS	Polarisation beam splitter
PC	Polarisation controller
PVA	Polyvinyl alcohol
RF	Radio frequency
SMF	Single mode fibre
SnO, SnO_2	Tin oxide
SNR	Signal to noise ratio
TBP	Time bandwidth product
WS_2	Tungsten disulphide
WDM	Wavelength division multiplexer
YDF	Ytterbium-doped fibre
YDFA	Ytterbium-doped fibre amplifier

LIST OF APPENDICES

CHAPTER 1

INTRODUCTION

1.1 Outline of the Report

This report consists of five chapters; introduction, literature review, methodology and work plan, results and discussion and conclusion and recommendation for future work.

In the introduction, important concepts such as mode-locking, operation of doped amplifier and supercontinuum generaton will be discussed, followed by the aims and objective, problem statements, scope and limitations cand contribution of the study.

The literature review discusses previous research on mode-locked fibre lasers including high power mode-locked fibre laser using mult-stage amplification and all-fibre mode-locked fibre laser. Some applications of the mode-locked laser will also be discussed.

The methodology and work plan describes the characterisation of the high power laser diode used for the amplifer and the construction of the laser cavity and the development of the EDFA, followed by the characterisation of the mode-locked pulses and the EDFA.

The result and discuttion describes the chracteristics of the mode-locked pulses and the output of the pulses after amplification. The pulse broadening from supercontinuum generation will be described.

The conclusion is the summary of this report and some recommendations for future work are also included.

1.2 General Introduction

Fibre laser is a variation of the standard solid-state laser. Instead of crystalline rods found in standard solid-state laser, the gain medium of the fibre laser is an optical fibre with rare earth dopants, such as ytterbium (Yb) and erbium (Er) (laserfocusworld, n.d.). The fibre laser is first demonstrated by Elias Snitzer in 1963 (Hecht, 2010). Since then, many developments were made to the fibre laser. Today, fibre lasers are able to generate high optical power output while offering more advantages than the typical lasers such as solid-state lasers or gas lasers. Fibre lasers are more compact and does not require alignment which makes them more practical in industrial applications (laserfocusworld, n.d.).
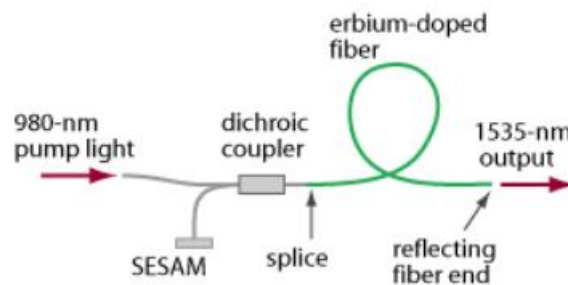
Figure 1.1. Fibre laser using Fresnel reflection as the output coupler and to form the resonator (Paschotta, 2020d).

One of the most important components of the fibre laser is the fibre laser resonator. To form the laser resonator with optical fibre, a reflector is required or a fibre ring laser can be constructed. Various type of mirrors can be used as a reflector. Some examples of the reflector used are a dielectric mirror attached to the cleaved fibre end. This is the simplest construction, but it is not durable. Utilising Fresnel reflection at the fibre end is often sufficient for a simple fibre laser construction. The Fresnel reflection also serves as an output coupler as shown in Figure 1.1. Other than Fresnel reflection, Dielectric coating at the fibre ends allows for the reflectivity at the fibre end to be manipulated. For commercial purposes, the fibre Bragg gratings are used (Paschotta, 2020d). Figure 1.2 shows an example of a fibre laser set up (FiberLabs Inc, 2020b).
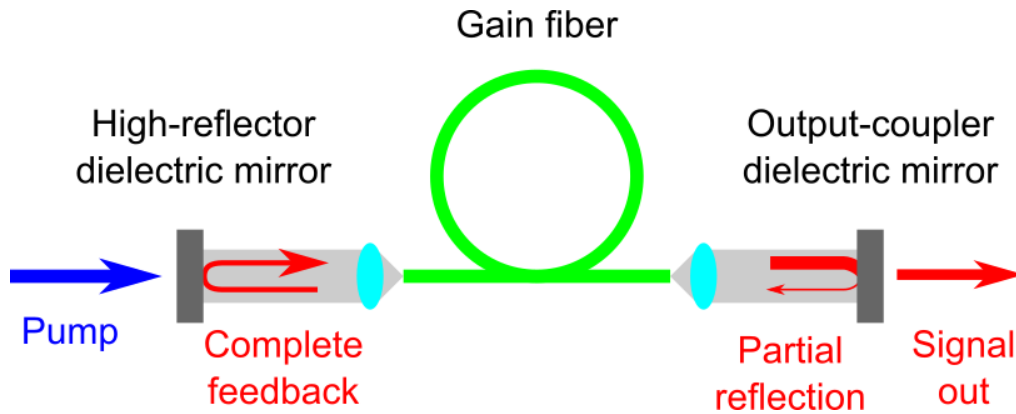
Figure 1.2 Example of fibre laser set up (FiberLabs Inc, 2020b).

Mode-locking is a method of obtaining ultrashort pulses, typically in few tens of picoseconds from laser (Paschotta, 2020l). When multiple longitudinal modes propagate in a laser, these modes oscillate independently which causes laser to be emitted continuously. This is the continuous wave (CW) operation of a laser as shown in Figure 1.3.
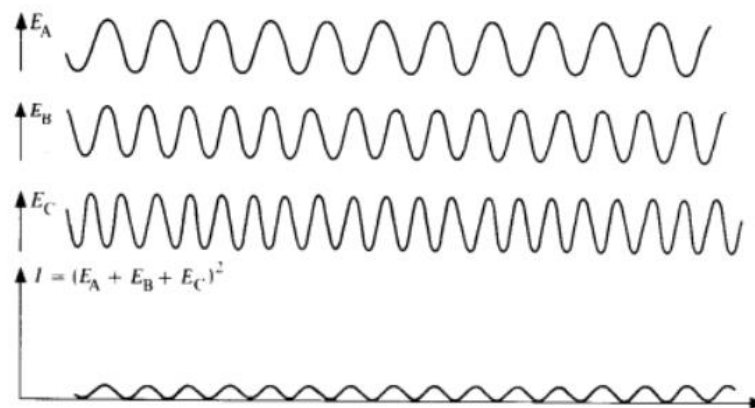
Figure 1.3 Continuous wave (CW) operation of a laser (Ennejah and Attia, 2013).

However, when there is a fixed phase relationship between the longitudinal modes, the various modes interfere to generate an output that is a series of pulse train. This is the mode-locked operation of the laser (Ennejah and Attia, 2013). The mode-locked operation of the laser is shown in Figure 1.4.
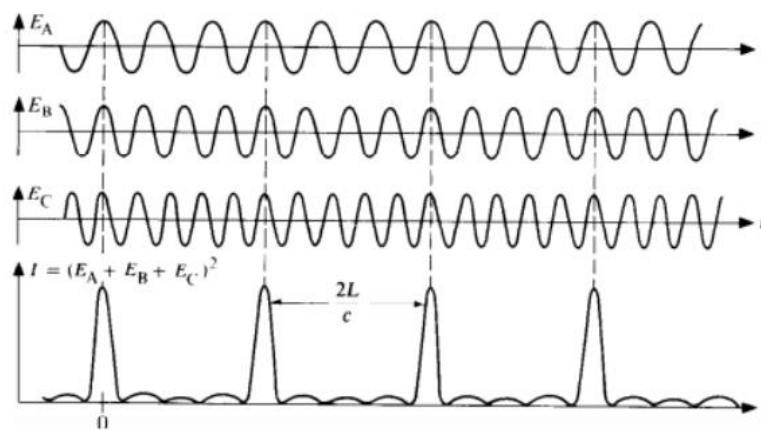
Figure 1.4. Mode-locked operation of the laser (Ennejah and Attia, 2013).

Fibre lasers can also be mode-locked. There are two mechanisms to achieve mode-locking; active mode-locking and passive mode-locking. Active components such as electro-optic modulator (EOM) or acousto-optic modulator (AOM) are used for active mode-locking. Passive mode-locking is done using passive components and do not require any external electrical or optical inputs. One of the ways to passively mode-lock a fibre laser is by using a saturable absorber in the laser cavity (Ennejah and Attia, 2013). The role of the saturable absorber in the laser cavity has not been investigated thoroughly but it is thought that the saturable absorber will help to initiate and stabilise the mode-locking regime (Churin, Kieu and Peyghambarian, 2012). Saturable absorbers are substances that absorb light but will have their absorption loss reduced at high optical intensity (Paschotta, 2020m)

Master oscillator power amplifier (MOPA) refers to the configuration consisting of a master laser (or seed laser) and an optical amplifier. A fibre amplifier, for example an erbium-doped fibre amplifier (EDFA) can be used. This variation of the MOPA system is called the master oscillator fibre amplifier (Paschotta, 2020i).
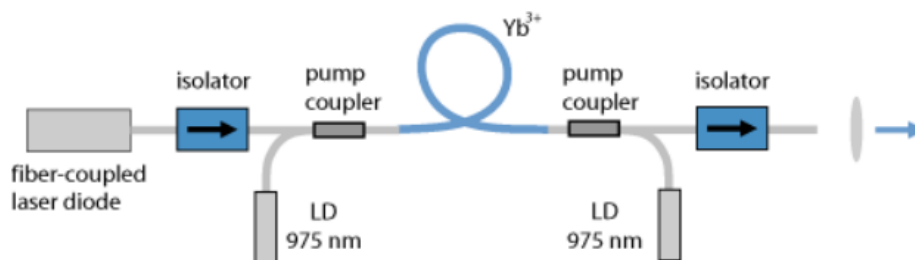
Figure 1.5. An example of the master oscillator fibre amplifier using an ytterbium-doped fibre amplifier (Paschotta, 2020i).

Figure 1.5 shows an example of the master oscillator fibre amplifier using an ytterbium-doped fibre amplifier. The MOPA system has several advantages. One of the advantages is easier to obtain the required performance (linewidth, wavelength tuning, beam quality, pulse duration etc) if the required output power is high. The second advantage is the system only require low-power optical components. The optical components can alter the low-power seed laser output to obtain the desired specification. The MOPA system will amplify the modified laser output after the optical components, giving the output the required performance and also have high optical power. It is also simpler to modulate a low-power laser output and then amplify it compared to direct modulation of a high-power laser. A combination of several amplifiers can increase the power of the output of existing lasers (Paschotta, 2020i).

The master oscillator fibre amplifier is often used for fibre-coupled output lasers, such as fibre lasers. The master oscillator fibre amplifier has a few advantages. High output power can be achieved due to high efficiency. The all fibre gain medium is easier to cool. Beam quality is from the fibre output is high. The gain of the doped-fibre is high, allowing for high amplification (Paschotta, 2020h).

1.3   Doped Fibre Amplifier

Doped fibre amplifiers are optical amplifiers which uses rare-earth-doped optical fibre as the gain medium. The doped fibre is pumped with a laser. The pump light propagates together with the signal to be amplified. Figure 1.5 shows the construction of an optical amplifier using ytterbium doped fibre as the gain medium.

Due to the small mode area and long fibre length, the doped fibre amplifier is able to achieve high gain (several tens of decibels). The doped fibre amplifier has large gain efficiency. Due to the small transition cross section, the saturation power of doped fibre amplifiers is higher (Paschotta, 2020c). The saturation power is inversely proportional to transition cross section as shown in Equation (1.1).

$$P_{sat} = \frac{Ah\nu}{(\sigma_{abs} + \sigma_{em})\tau} \tag{1.1}$$

where A is the mode field area, ν is the frequency σ_{abs} and σ_{em} are the absorption and emission cross-section respectively and τ is the upper-state lifetime (Paschotta, 2020n). Therefore, the energy stored in the doped fibre amplifier is higher and thus, the power that can be extracted is also higher. The amplification of mode-locked laser is the same for the amplification for continuous wave laser (Paschotta, 2020c).
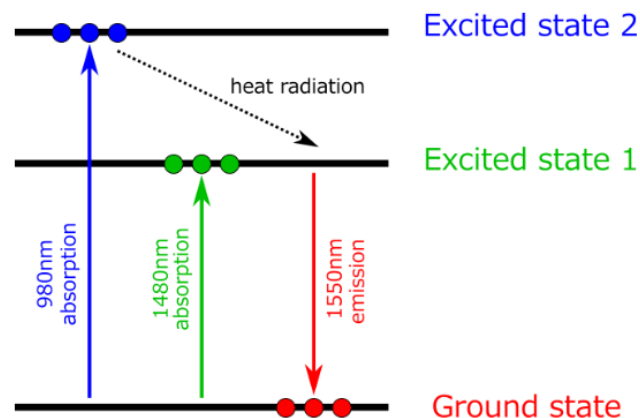
Figure 1.6. Energy band diagram of erbium (FiberLabs Inc, 2020a).

The working principle of the doped fibre amplifier will be explained using the EDFA as an example. The energy band diagram of erbium is as shown in Figure 1.6. When the EDFA is pumped at 980 nm, the Er ions are excited to the second excited state (excited state 2 in Figure 1.6). The lifetime of excited state 2 is short, the Er ions will then decay to the excited state 1. These conditions allow the ground state Er to be pumped to the excited state 2 is always at low density. When pump power is sufficient, the Er ions will be accumulated at the excited state 1 which has longer lifetime at approximately 10 ms. This creates a population inversion between excited state 1 and the ground state. The input signal of 1550 nm will cause stimulated emission and the input signal will be amplified in this process (FiberLabs Inc, 2020a). The EDFA is pumped with the 980 nm so that it is operated in the high saturation region so that the output power will be highest. The saturated power is higher if the Er ions are pumped to excited state 2 because excited state 2 has shorter lifetime. Saturation power is inversely proportional to excited state lifetime, as shown in Equation (1.1).

The doped fibre amplifier can be pumped in either the forward or backward direction or bidirectionally (as show in Figure 1.5). The direction of pumping does not influence the small-signal gain, but it affects the power efficiency and the noise characteristics. Bidirectional pumping can be used to obtain high power, low noise and high power efficiency (Paschotta, 2020c).

The fibre amplifier can also be used in a multi-step amplification instead of single-step amplification. A sequence of several amplifiers is used in the multi-step amplifier. The first few amplifiers are called the pre-amplifier and the last amplifier is called the power amplifier. Splitting the amplifier to different stages allows for better performance by using a large mode field area for the power amplifier to reduce non-linear effects and a small mode field area for the pre-amplifier for better gain efficiency. The pre-amplifiers and power amplifier can be independently optimised to avoid distortion to the pulse. This is important in amplification of mode-locked pulses. Optical components can also be inserted in between the pre-amplifiers and power amplifier to alter the pulse (Paschotta, 2020a). The MOPA system can be a single-step amplification or multi-step amplification.

1.4   Supercontinuum Generation

The Kerr effect is the change of refractive index of a material in due to strong electromagnetic field. For optical waves, the field is oscillation. Therefore, the change in refractive index, Δn, is proportional to the intensity, I

$$\Delta n = n_2 I$$

where n_2 is the non-linear index which quantifies the Kerr non-linearities. This quantity is medium dependent. The Kerr effect is a non-linear optical effect because the change in refractive incex is proportional to the square of the electric field strength. This effect is weker than the Pockels effect which is proportional to the electric field strength (Paschotta, 2020f).

A strong optical pules is able to undergo self-phase modulation when propagationg trough a dispersive medium due to the Kerr effect. This can cause a time-dependent phase shift on the pulse according to the change of the pulse intensity. This results in the broadening or compression of the pulse, depending on the Kerr non-linearity of the medium (Paschotta, 2020o).

As the result of self-phase modulation, a soliton pulse propagating through a medium can undergo supercontinuum generation which is undesirable. Supercontinuum generation is a phenomena when a laser light pulse is converted to a light broad bandwidth. The resultant light has low temporal coherance (the spatial coherence is maintained) and has a super-wide continuous optical spectrum. The mechanism behind the supercontinuum generation is dependent on the nature of the medium but for a soliton pulse propagating through an optical fibre, the supercontiuum generation is maily due to self-phase modulation induced by the high intensity of the pulses. This result in the loss of the mode-locked laser pulses. This is a major challenge in designing a mode-locked fibre laser (Paschotta, 2020q).

1.5   Importance of the Study

Fibre lasers have a number of qualities which make them attractive to be made into mode-locked laser. The gain medium of the fibre laser is a rare-earth-doped optical fibre which has a large gain bandwidth which allows for a low pulse width. The doped fibre also has high efficiency which allows lasing to occur at a low pump power. This combined with the relatively low cost of manufacturing (compared with bulk laser) makes the mode-locked fibre laser very practical in industrial applications.

The mode-locked fibre laser is largely used in telecom applications due to its long-term reliability and low cost and due to fibre-coupled output, it is compatible with many telecom systems (Paschotta, 2020j).

The mode-locked fibre laser typically generates optical output power in the range of hundreds of milliwatts (Ahmed et al., 2016; Li et al., 2016). To obtain high power (exceeding 1 W), it is necessary to use the MOPA system to amplify the output optical power (Chen et al., 2009).

1.6   Aim and Objectives

Mode-locked lasers are widely used in many industry applications. A mode-locked fibre laser is the most practical for industrial purposes due to its relatively cheap cost and ease of use compared to bulk laser while being able to produce high optical output power. The mode-locked fibre laser system often does not output high optical power. The MOPA system can be used to amplify the laser output but non-linear effects caused by the fibre amplifiers can alter the mode-locked pulse characteristics. Therefore, the effects of integrating the MOPA system into the mode-locked fibre laser system has to be investigated. Due to the high intensity of the mode-locked pulses, non-linear effects, particularly supercontinuum generation due to self-phase modulation as the pulses propagate through the optical fibre. This effect needs to be understood and characterised to design a mode-locked fibre laser without any undesirable effects.

1.7 Scope and Limitation of the Study

This project mainly focuses on designing a compact fibre laser module that can produce a stable high-power mode-locked laser output. This involves setting up the laser diode to pump the gain medium and building the laser cavity. The appropriate saturable absorber needs to be selected. Since the role of the saturable absorber in the mode-locking regime is not deeply understood, the only way to select the appropriate saturable absorber is by testing multiple materials for the saturable absorber. Some commonly used materials used as as saturable absorbers are graphene oxide (GO), molybdenum disulphide flakes (MoS_2) and tin oxide (SnO, SnO_2).

To save resources, commercially available EDFA will be used along side with custom made EDFA to obtain the required output power. Therefore, multiple step amplification will be done. The pulse width and repetition rate is also not a concern. The pulse width of a few femtoseconds and the repetition rate of a few megahertz are acceptable. The focus of this project is not to obtain a high repetition rate andd a very short pulse.

1.8 Contribution of the Study

In this research, a high power mode-locked fibre laser wil be developed from optical equipments available in the lab. The main motivation of this research is to develop another mode-locked laser source to be used for the experiments in the lab. The mode-locked fibre laser system has also several unique advantages over bulk laser, namely, the beam size can be much smaller. This is extremely beneficial for polymer waveguide writing system where a high resolution is desired. The mode-locked fibre laser system also has the added advantage of being cheaper and less bulky compared to conventional solid state mode-locked lasers.

CHAPTER 2

LITERATURE REVIEW

2.1   Introduction

In the literature review, past research on mode-locked fibre laser will be discussed. This includes research on high power and ultrashort pulses. Mode-locked fibre laser using saturable absorber and all-fibre mode-locked mode-locked laser will be investigated. The mode-locked fibre laser with MOPA system with both single-step and multi-step amplification will also be discussed. The applications of mode-locked laser will be discussed.

2.2   Mode-Locked Fibre Laser Using Saturable Absorber

Mode-locked fibre laser has been demonstrated by many research groups. One such group in the Photonics Research Centre, Universiti Malaya has demonstrated mode-locked fibre laser using MoS_2 as the saturable absorber and erbium-doped fibre (EDF) as the gain medium. The experimental setup is shown in Figure 2.1. The laser cavity consists of 1.8 m long EDF and 5 m long standard SMF. The EDF is pumped with a 980 nm laser diode via the 980/1550 nm wavelength division multiplexer (WDM). An isolator is placed in the laser cavity to prevent back reflection. The laser output is delivered through a 95/5% output coupler. 95% of the light generated is feedback into the laser cavity. The polarisation controller (PC) adjusts the polarisation state within the cavity. The 5% output is analysed with an optical spectrum analyser (OSA) and a photodetector which is connected to an oscilloscope.

Figure 2.1. Setup of the mode-locked fibre laser with MoS_2 as the saturable absorber and EDF as the gain medium (Ahmed et al., 2016).

The MoS_2 flakes are prepared by exfoliation of bulk MoS_2 crystal. The bulk crystal is mixed into dimethylformamide (DMF) solvent. DMF solvent is used because it has similar surface energy with MoS_2. The exfoliation is done by ultra-sonification of the solution for 24 hours. The resultant dispersion is centrifuged for one hour. This sediments the larger MoS_2 flakes. The upper 80% of the dispersion consists of few-layer MoS_2 flakes and is decanted. To form free standing MoS_2 – polymer composite film, the solution is mixed with polyvinyl alcohol (PVA) and deionised water. The solution is stirred with a magnetic stirrer and heated continuously at 80°C for approximately 7 hours. The reduced solution is poured onto a glass substrate and is dried in an oven to form a ~40 µm thick free-standing composite film. Raman spectroscopy shows that this process produces few-layer thick MoS_2 flakes.

From this experimental setup, the laser operation is initiated at pump power of 17 mW. The laser first began with CW operation. The soliton pulse was achieved at 25 mW and by controlling the polarisation state using the PC. Stable mode-locked pulses are achieved at 170 mW. The MoS_2 film did not sustain any thermal damage. The pulse repetition rate is 27.1 MHz which is determined by the 7.3 m cavity length. Figure 2.2 shows the pulse train of the mode-locked pulse.
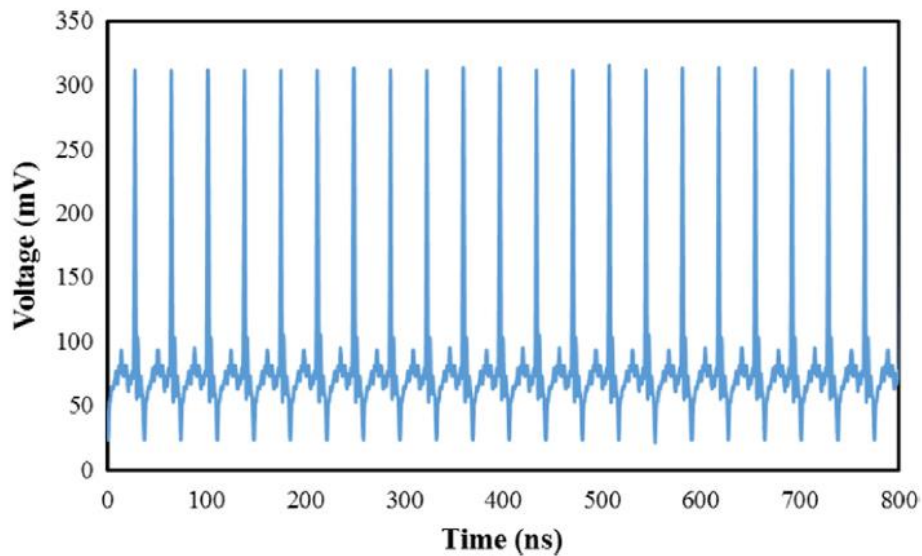
Figure 2.2. The oscilloscope trace showing the mode-locked pulse train (Ahmed et al., 2016).
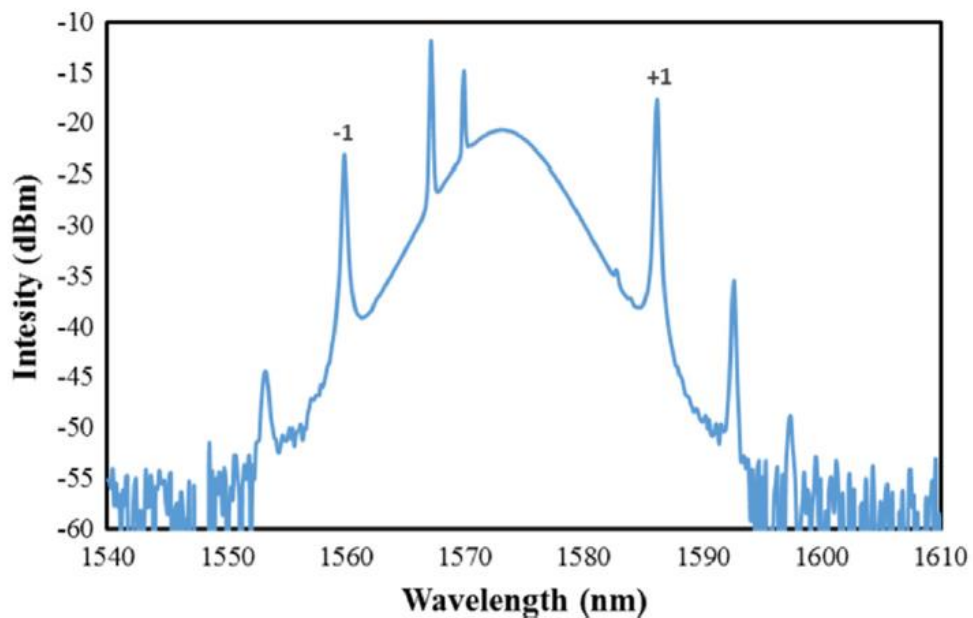
Figure 2.3. Optical spectrum of the mode-locked pulse (Ahmed et al., 2016).

Figure 2.3 shows the optical spectrum of the mode-locked pulse. The pulse has a centre wavelength of 1573.7 nm with peak power -20.1 dBm with full width at half maximum (FWHM) of 7.3 nm. Kelly sidebands are also present due to the dispersion of the cavity. Based on the sideband separation, the actual dispersion of the cavity is -0.118 ps^2 (negative dispersion indicates that the cavity dispersion is anomalous).
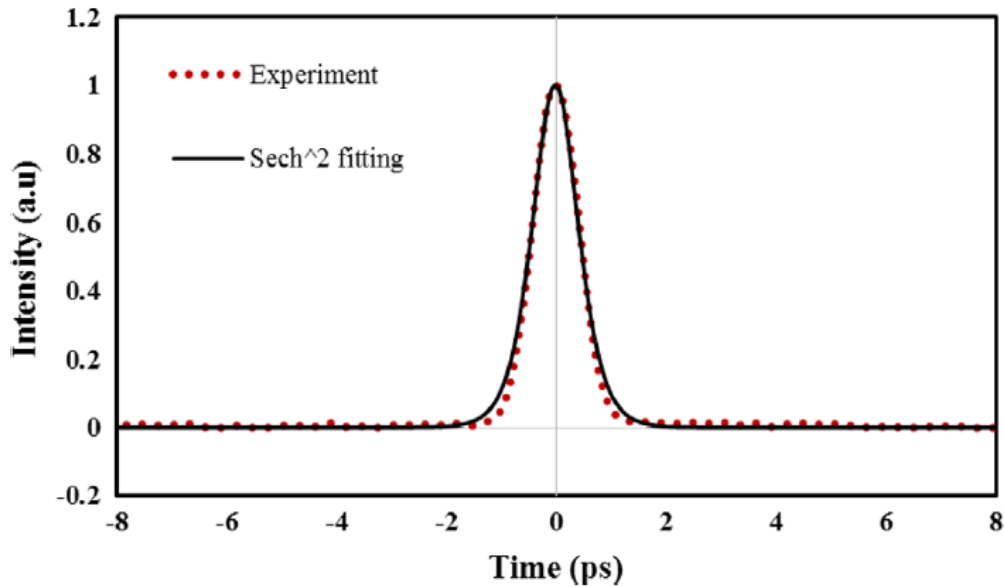
Figure 2.4. Autocorrelator trace of the mode-locked pulse (Ahmed et al., 2016).

Figure 2.4 shows the autocorrelator trace of the mode-locked pulse. The pulse width is 630 fs. The pulse energy is 0.141 nJ with peak power of 210 mW at pump power of 170 mW.
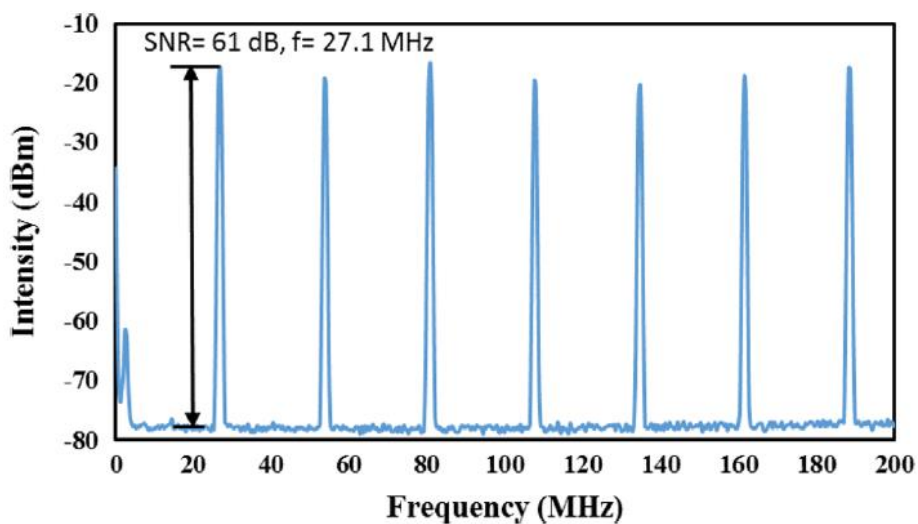
Figure 2.5. Radio-frequency (RF) spectrum of the mode-locked pulse (Ahmed et al., 2016).

Figure 2.5 shows the RF spectrum of the mode-locked pulse. The spectrum shows that higher order modes are present without any signs of Q-switching instability. The signal to noise ratio (SNR) is 61 dB.
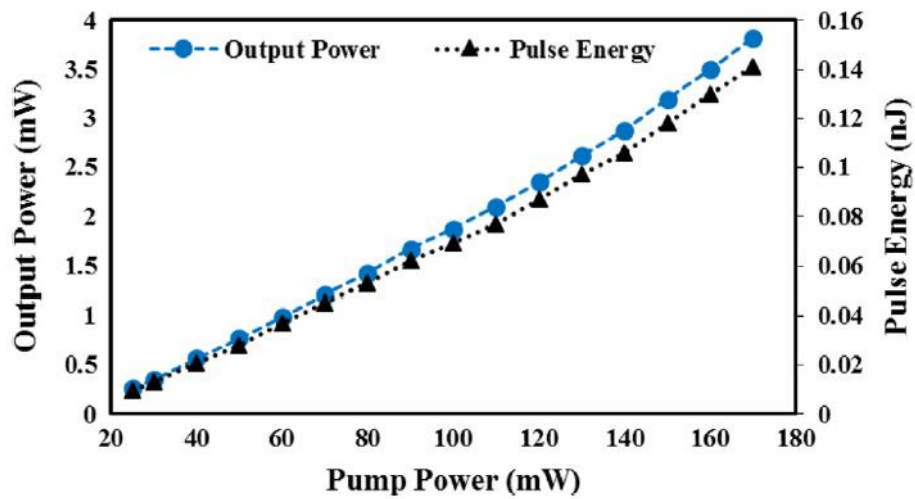
Figure 2.6. Average output power and pulse energy at different pump power (Ahmed et al., 2016).

Figure 2.6 shows the average output power and pulse energy at different pump power. The average output power and pulse energy increases with pump power. Therefore, this research shows that MoS_2 film is a good candidate to produce mode-locked pulses (Ahmed et al., 2016). This is the simplest setup for mode-locked fibre laser using 2D material as the saturable absorber. The MoS_2 film is simply sandwiched between two fibre ferules.
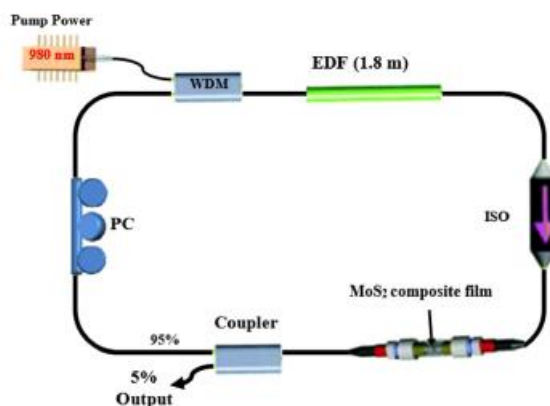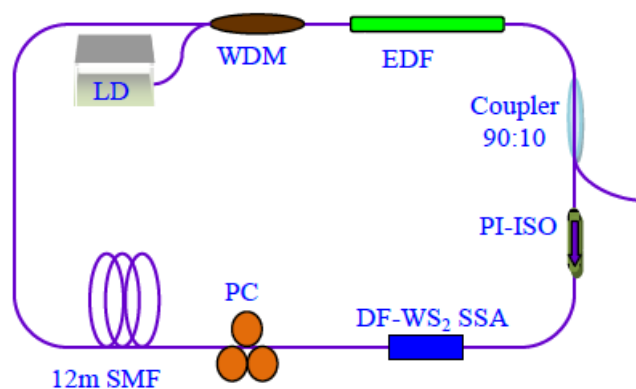

Figure 2.7. Setup of the mode-locked fibre laser using WS_2 as the saturable absorber and EDF as the gain medium (Li et al., 2016).

In addition, mode-locked fibre laser has also been demonstrated by Li et al in 2016 using tungsten disulphide (WS_2) with EDF as the gain medium. Figure 2.7 shows the setup of the mode-locked fibre laser using WS_2 as the saturable absorber and EDF as the gain medium used by Li et al. The setup is almost identical to the one used by Ahmad et al. The length of the EDF used here is 4 m and the length of the SMF is 12 m. The total length of the cavity (including all the optical components) is 20.3 m. The output coupler used is a 90/10% output coupler. 90% of the light is feedback into the laser cavity. The net cavity dispersion is calculated to be -0.35 ps^2.

The WS_2 saturable absorber is prepared by first sonicating and centrifuging WS_2 powder in water-ethanol. The resultant solution contains WS_2 nanosheets. A D-shaped fibre with fibre-core boundary to D-shaped surface of 2 µm is fabricated. The D-shaped fibre is sealed in the box filled with the WS_2 nanosheets solution.
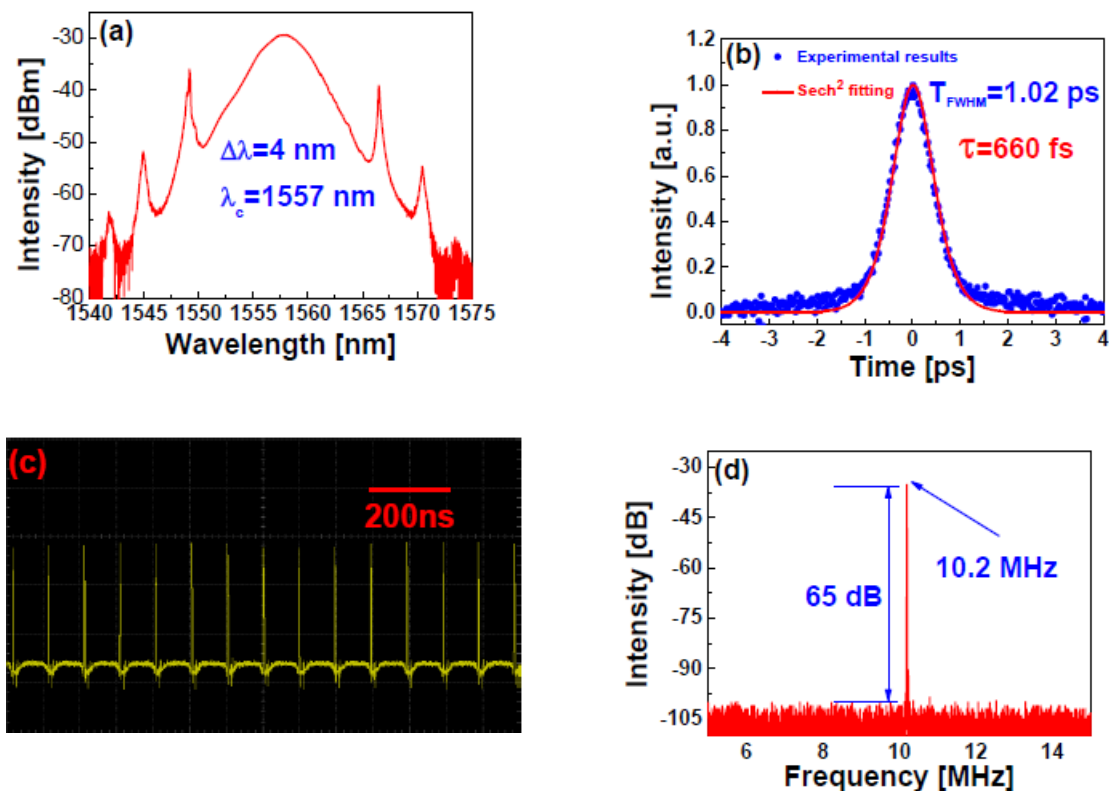
Figure 2.8. Fundamental mode-locking results: (a) optical spectrum, (b) autocorrelation trace, (c) oscilloscope trace and (d) RF spectrum (Li et al., 2016).

Figure 2.8 shows the results of the fundamental mode-locking obtained from the experiment. Fundamental mode-locking is achieved with pump power of 14.4 mW. The centre wavelength is 1557 nm with spectral width 4 nm. Kelly sidebands are also observed. From the autocorrelation trace, the pulse width is 660 fs. The oscilloscope trace shows that pulses with uniform intensity occur at the interval of 98 ns. The repetition rate is 10.2 MHz. The SNR is 65 dB.
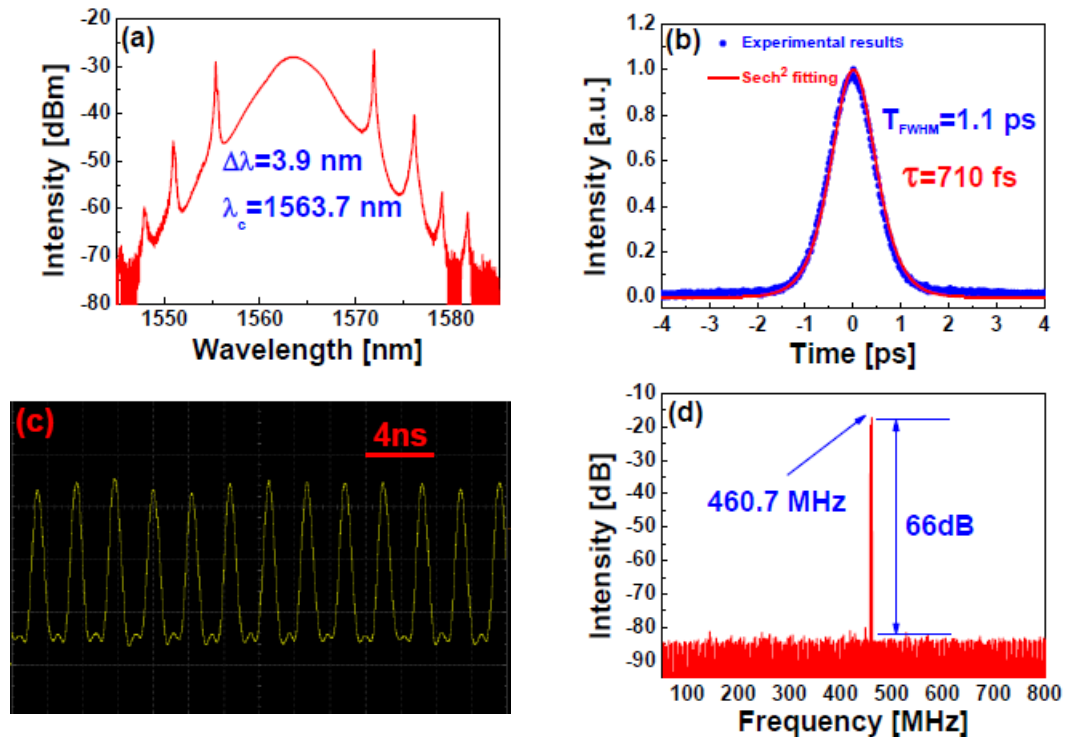
Figure 2.9. Higher order mode-locking results: a) optical spectrum, (b) autocorrelation trace, (c) oscilloscope trace and (d) RF spectrum (Li et al., 2016).

Figure 2.9 shows the results of the higher order mode-locking. Higher order mode-locking is achieved with pump power of 350 mW. The centre wavelength is 1563.7 nm with spectral width of 3.9 nm. Kelly sidebands are also present. From the autocorrelation trace, the pulse width is 710 fs. The oscilloscope trace shows that the pulses occur at an interval of 2.17 ns which corresponds to repetition rate of 460.7 MHz. The RF spectrum shows that the SNR is 66 dB.

Therefore, this experiment demonstrates that both fundamental and higher order mode-locking can be achieved using WS_2 nanosheets as the saturable absorber. The advantage of using WS_2 nanosheets in solution is that it prevents thermal degradation and oxidation of WS_2 which will disrupt the stability of the mode-locking regime (Li et al., 2016).

The two experiments discussed have demonstrated that mode-locking can be achieved using a variety of 2D material as the saturable absorber. The characteristics of the mode-locked pulse are highly dependent on the net cavity dispersion. The saturable absorber plays a role in initiating and stabilising the mode-locking regime. The two mode-locked fibre laser system demonstrated are able to provide stable, mode-locked laser output. However, the output optical power is only a few hundreds of milliwatts. To obtain higher optical power, the MOPA system has to be integrated.

2.3   Mode-Locked Fibre Laser with MOPA System

The average power of mode-locked laser is limited by the onset of non-linear effects such as self-phase modulation and stimulated Raman scattering due to the small mode field area and long fibre length. The non-linear effects can be suppressed by increasing mode field area, but this deteriorates beam quality. However, using a MOPA configuration eliminates these issues (Chen et al., 2009).
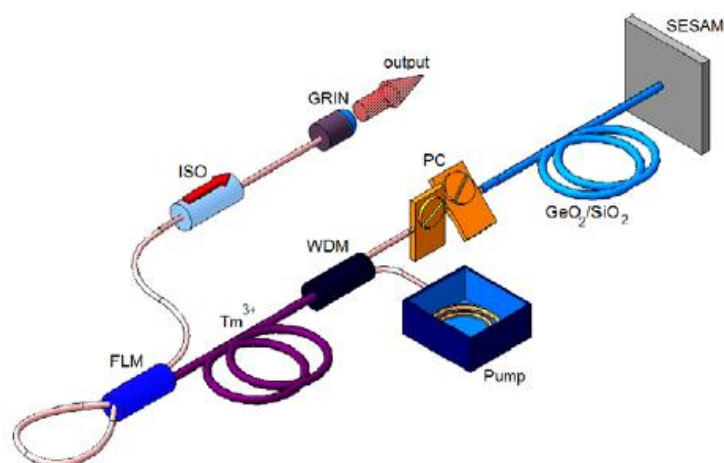
Figure 2.10. Mode-locked thulium (Tm) doped fibre laser with dispersion management (Krylov et al., 2013).

Figure 2.10 shows the mode-locked thulium doped fibre laser. The fibre laser has a liner cavity with a 68 cm long Tm-doped fibre terminated with a fibre looped mirror (FLM) and a semiconductor saturable absorber mirror (SESAM), which initiates and maintains the mode-locking regime. The TM-doped fibre is pumped with a CW erbium-ytterbium fibre laser with wavelength of 1560 nm with optical power of 250 mW. The germanium-silica glass (GeO_2 /SiO_2) fibre is used to control the dispersion of the cavity. The polarisation controllers (PC) placed before the SESAM controls the polarisation state in the cavity so that a single-pulse mode-locked lasing is achieved. The graded-index (GRIN) collimator and isolator (ISO) are placed at the end of the FLM for the laser output.

The stable mode-locked output is observed when the GeO_2/SiO_2 fibre is less than 1 m. The net cavity dispersion changes from +0.15 ps^2 to -0.11 ps^2 when the net cavity length is changed from 2.7 m to 1.7 m by shortening the germanium-silica fibre.
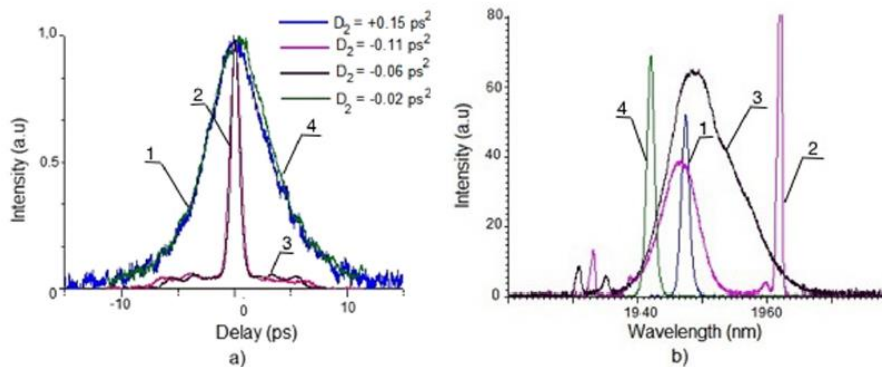
Figure 2.11. Output characteristic of the mode-locked thulium doped fibre laser: (a) Autocorrelation traces and (b) optical spectra at different net cavity dispersion (Krylov et al., 2013).

Figure 2.11 (a) shows the autocorrelation traces and (b) shows the optical spectra of the mode-locked thulium-doped fibre laser. When the GeO_2/SiO_2 fibre is 1 m and 0.42 m, the net cavity dispersion is +0.15 ps^2 (blue curve) and -0.02 ps^2 (green curve) respectively. The laser output shows a

Gaussian pulse shape. The spectral width is 1.44 nm and 1.45 nm respectively. The pulse duration is 4.8 ps for both. The time-bandwidth product is roughly 0.55 for both. The transform limit for a Gaussian pulse is 0.441. Time-bandwidth product of the two pulses are close to the transform limit which shows that the spectral width is minimum. The pulse width does not decrease with pump power. When the GeO_2/SiO_2 is 0.26 m (pink curve) and 0.07 m (black curve), the net cavity dispersion is -0.11 ps^2 and -0.06 ps^2 respectively. The spectral width is 11.5 nm and 6.3 nm respectively. The pulse duration is 720 ps for both. In the case of the 0.07 m long GeO_2/SiO_2 fibre, the optical spectrum shows sharp Kelly sidebands. For near-zero dispersion (the black curve), the pulse does not follow soliton behaviour. The experimental results show that the mode-locked thulium-doped fibre laser is able to generate a stable mode-locked output. The pulse duration can be altered by adjusting the net cavity dispersion.
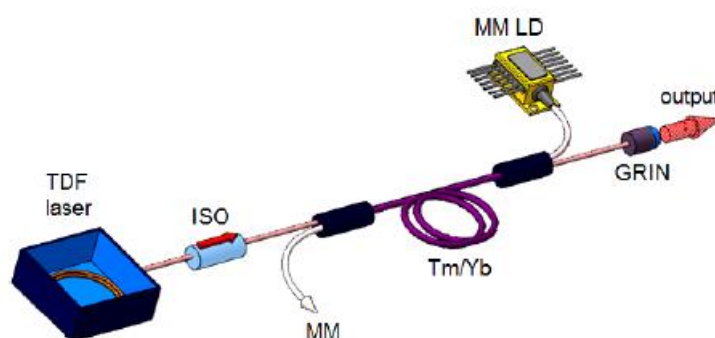
Figure 2.12. The thulium and ytterbium co-doped amplifier for the mode-locked thulium-doped fibre laser (Krylov et al., 2013).

Figure 2.12 shows the MOPA setup with the mode-locked thulium-doped fibre laser. The gain medium of the fibre amplifier is a 5 m long silica-alumina-ytterbium and thulium co-doped (Tm/Yb) fibre. The pump is a 9 W or 17 W laser diode which is coupled into the multimode waveguide of the Tm/Yb fibre. The output is pigtailed into a GRIN collimator. The length of the GeO_2/SiO_2 fibre is varied from 1 m to 0.3 m.
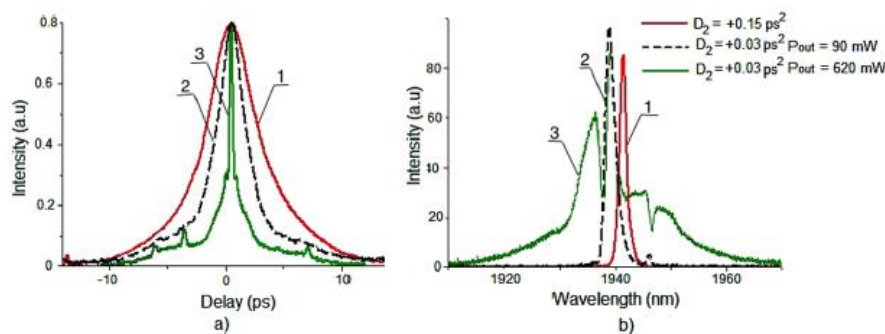
Figure 2.13. Output characteristic of the amplified pulse: (a) Autocorrelation trace and (b) optical spectra (Krylov et al., 2013).

Figure 2.13 (a) shows the autocorrelation trace of the amplified pulse and (b) shows the optical spectra. The pulse shape for the amplified pulses are Gaussian. In the case of a 1 m long GeO_2/SiO_2 fibre (the red curve) the pulse width is 3.4 ps with spectral width of 2.2 nm. Average power is 1.1 W at pump power of 9 W. By increasing the pump power to 17 W, the output power reached 2 W. Therefore, using the combination of a mode-locked fibre laser and a MOPA system, mode-locked pulses with average power of 2 W can be obtained. Using dispersion compensation, stable Gaussian pulses are can be obtained (Krylov et al., 2013).

The experiment by Krylov et al (2013) demonstrated a single-step amplification to obtain a 2 W mode-locked pulses. To obtain higher optical output power, multi-step amplification can be used.
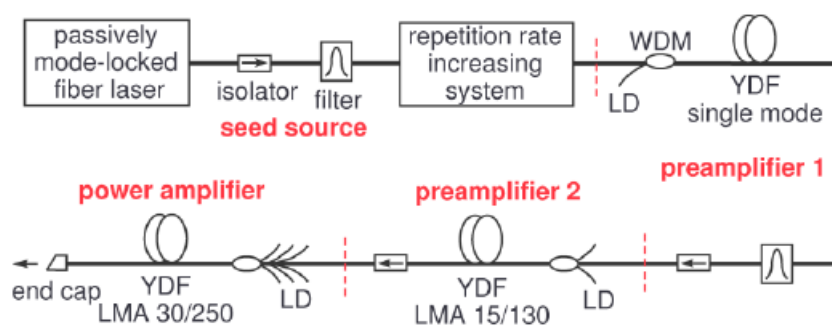
Figure 2.14. High-power mode-locked fibre laser setup with a three-step amplification (Chen et al., 2009).

Figure 2.14 shows the high-power mode-locked fibre laser with three-step amplification. The seed laser is a mode-locked ytterbium-doped fibre laser with average power of 20 mW, pulse width of 13 ps and repetition rate of 59.8 MHz. The bandpass filter at the seed laser output eliminates amplified spontaneous emission. The repetition rate increasing system increases the repetition rate by eight times. Increasing the repetition rate suppresses non-linear effects by decreasing peak power while maintaining average power. After increasing the repetition rate, the output is amplified by a YDFA. The second stage amplification is done with a double clad YDFA pumped by two 20 W laser diodes with wavelength of 976 nm. The last stage of amplification is done by a double clad YDFA pumped by six 20 W laser diodes with wavelength of 976 nm. The output is angled to prevent back reflection. The amplifiers are forward pumped to prevent damage to the laser diodes.
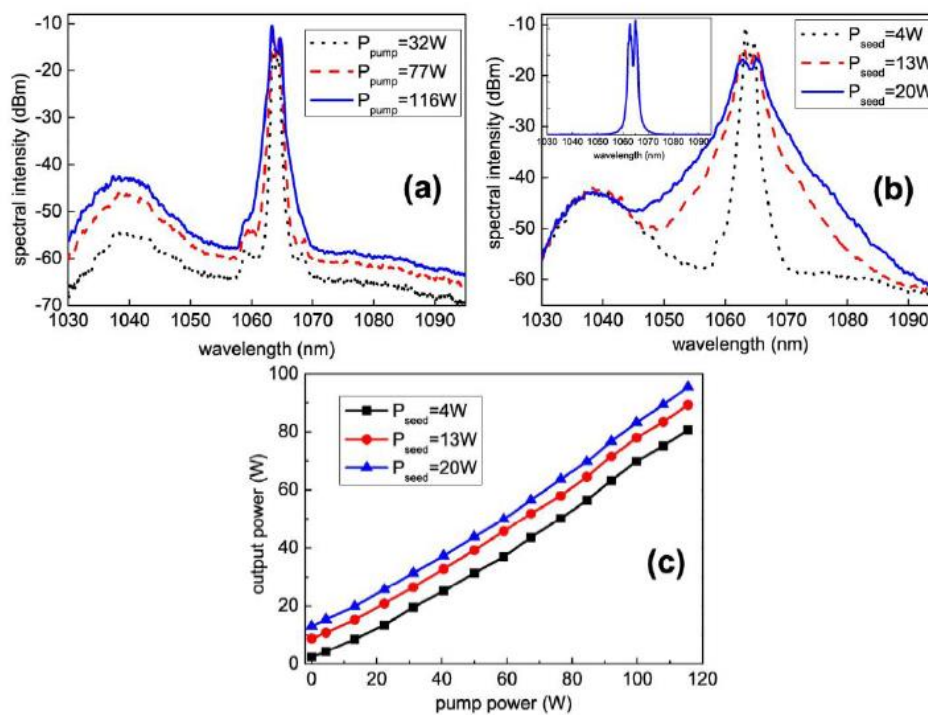
Figure 2.15. Output characteristics of the amplified pulse after the power amplifier: (a) Optical spectra at various total pump power , (b) Optical spectra at various seed laser power and (c) Output power versus various seed power (Chen et al., 2009).

Figure 2.15 (a) the optical spectra of the amplified pules after the power amplifier at various pump power, (b) shows the optical spectra at various seed laser power and (c) shows the output power at various seed power. Spectral broadening is observed with increasing seed laser power. This is attributed to the broadening of the spectrum of the seed laser itself. The output power increases with pump power. Maximum output power of 96 W is obtained at total pump power of 156 mW and seed laser power of 20 W. The pulse width measured using an autocorrelator is 16 ps (Chen et al., 2009).

2.4 All-Fibre Mode-Locked Fibre Laser

Besides using a saturable absorber, mode-locking can also be achieved by using the non-linear properties of the fibre. This has been demonstrated by Duling in 1991 using a ring laser and a non-linear amplifying loop mirror (NALM).
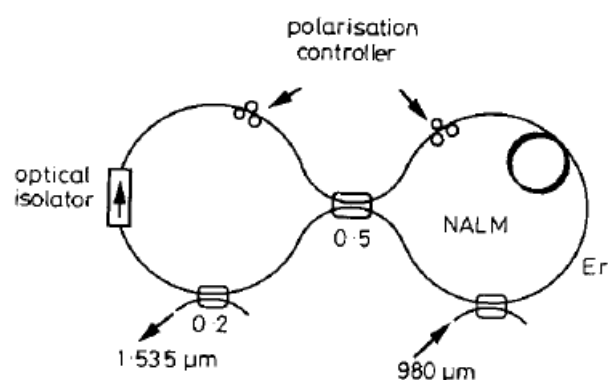
Figure 2.16. Setup of the fibre laser using EDF as the gain medium and NALM (Duling, 1991).

Figure 2.16 shows the mode-locked fibre laser using NALM with EDF as the gain medium. The NALM comprises of a 50% output coupler, EDF and a WDM pump coupler. The output of the NALM is connected to an isolator and the output of the isolator is connected into the input of the NALM. The operating characteristics of the laser are highly dependent on the length of the fibre as the cavity dispersion is dependent on the length. The NALM is also responsible for pulse shaping. The pulse produced in the cavity will be broadened as it travels along the cavity and the pulse will be shaped by the NALM.
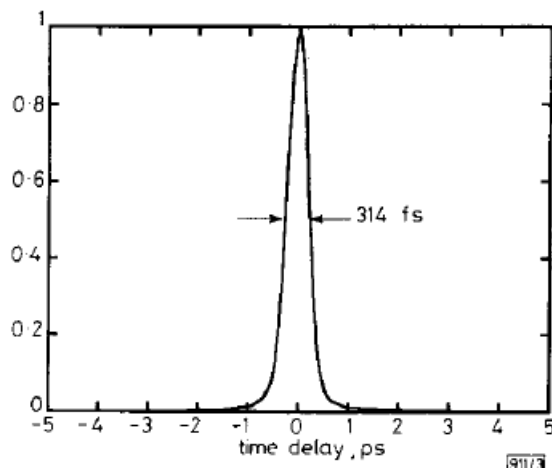
Figure 2.17. Autocorrelation trace of the mode-locked fibre laser using NALM with non-linear fibre length of 1.2 m (Duling, 1991).

Figure 2.17 shows the autocorrelator trace of the mode-locked fibre laser using the NALM. The autocorrelator trace shows that pulse width is 314 fs. The pump power to achieve mode-locking is 200 mW. This is higher than typical mode-locked fibre laser using saturable absorber but the author reported that this could be due to the old design of the EDF which has lower gain efficiency.
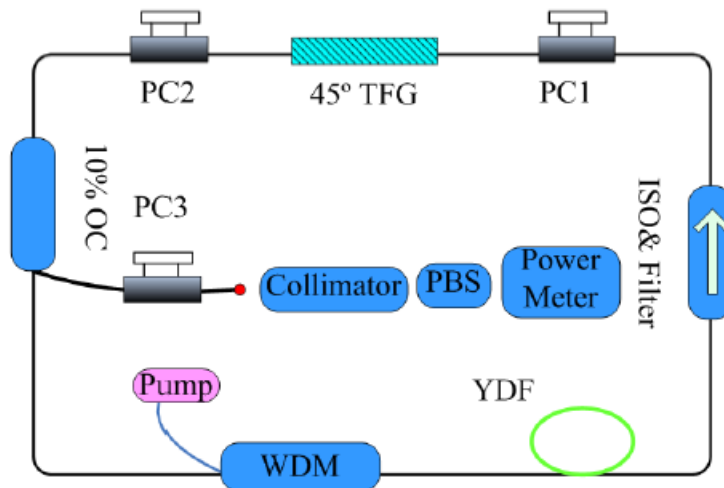
Figure 2.18. Setup of the mode-locked fibre laser using 45° tilted fibre grating (45TFG) (Liu et al., 2012).

Another way of achieving mode-locking with an all-fibre setup is using a 45TFG. The 45TFG has many merits that make it attractive in the application of generating mode-locked pulses. The 45TFG has high polarisation dependent loss, high damage threshold and high operation bandwidth.

Figure 2.18 shows the setup of the mode-locked fibre laser using 45TFG. The 45TFG is fabricated using UV inscription. The gain medium used by Liu et al is an ytterbium-doped fibre (YDF). The cavity comprises of YDF and SMF. The total cavity length is 7 m. A 980 nm laser diode is used as the pump. The 45TFG and the two PCs function similar to the saturable absorber. The polarisation state of the output is studied using the polarisation beam splitter (PBS).

The 45TFG causes light to leave it in linear polarisation state. The rotation angle is proportional to the area of the polarisation ellipse. Linearly polarised light does not experience any rotation. Adjusting PC1 changes the polarisation to elliptical polarisation. Due to Kerr effect in the medium, self-phase modulation and cross-phase modulation occurs. The polarisation state of the light evolves along the length of the cavity. The polarisation state is non-uniform due to the intensity dependence of the Kerr effect. PC2 forces the polarisation state of the centre of the pulse to be identical to that of the 45TFG. Thus, the 45TFG lets the centre of the pulse pass and blocks the pulse wings.
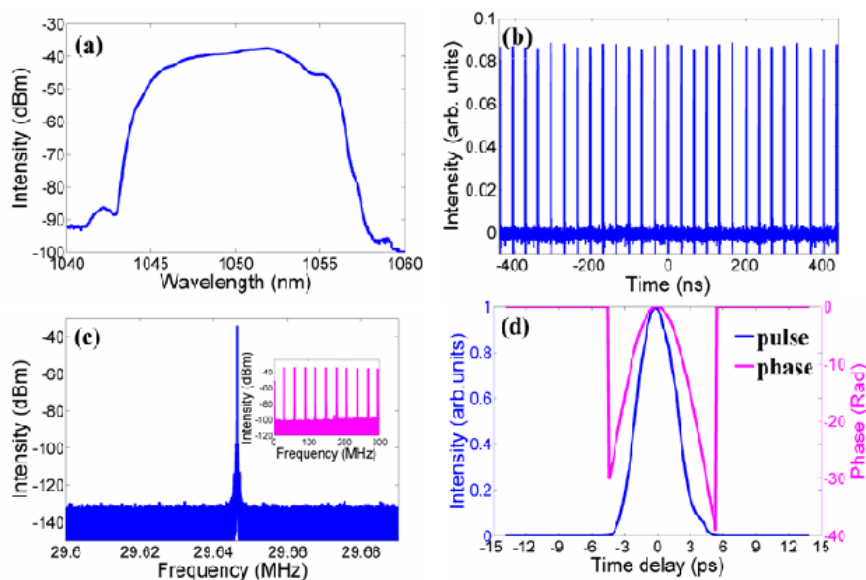
Figure 2.19. Results of the mode-locked fibre laser using 45TFG: (a) optical spectrum, (b) oscilloscope trace, (c) RF spectrum and (d) phase and pulse profile (Liu et al., 2012).

Figure 2.19 shows the experimental results of the mode-locked fibre laser using 45TFG. By adjusting the PCs, mode-locking is achieved at 196 mW. The centre wavelength is 1050 nm with spectral width of 9 nm. The pulse interval is 33.7 ns. The wide spectrum with steep edges is typical of normal dispersion pulse. The repetition rate is 29.646 MHz. The RF spectrum shows no Q-switching instabilities. The SNR is 80 dB which shows that the mode-locking is stable. The pulse width is 4 ps (Liu et al., 2012).

2.5　Applications of Mode-Locked Fibre Laser

As mentioned previously, mode-locked lasers have a variety of applications. It is commonly used in multiple high-precision measurement techniques, non-linear optics, micromachining and many more.

One of the applications of mode-locked laser is Z-scan. The Z-scan is a measurement technique to measure the strength of Kerr non-linearity of a material, relying on the self-focusing. It is used to characterise the non-linear optical properties of a material.
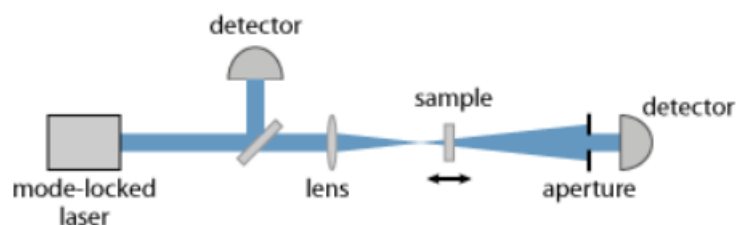
Figure 2.20. Setup of z-scan measurement (Paschotta, 2020r).

Figure 2.20 shows the setup of the z-scan measurement. The Kerr effect is the change of refractive index of a material as light propagates through it. This change of refractive index is dependent on the intensity of the light (Paschotta, 2020g). Therefore, to deliver high intensity to the material, a mode-locked laser is used because it is able to deliver high intensity compared to a CW laser due to high pulse intensity (Paschotta, 2020k). The sample under investigation is moved through the focus of the laser beam. The beam radius is measured at a point behind the focus as the function of the sample position. These quantities are affected by the self-focusing effect. If the non-linear index is positive and the sample is placed behind the focus, the beam divergence is reduce, thus, increasing the detector signal. On the other hand, if the sample is moved in front of the focus, the beam divergence is increase, thus, reducing the detector signal. Based on the dependence of the signal strength with sample position, the non-linear index can be calculated.

Due to the high pulse intensity of the mode-locked laser, non-linear effects can be induced. One such non-linear effect is non-linear absorption. This is particularly useful in processing transparent materials which do not have any linear absorption coefficient at the wavelength of the mode-locked laser. Using the mode-locked laser for processing transparent material has a few advantages. First, the material alteration is confined to the focus of the laser, allowing for high precision. Next, the absorption process is independent of material, allowing devices to be fabricated with different substrate. Third, the mode-locked laser can be used to fabricate optical motherboard, where all the interconnects are fabricated separately, before or after bonding several photonic devices to a single transparent substrate.

Micromachining of transparent material must involve non-linear absorption because there are no electronic transitions are allowed at the energy of the incident photon. For the non-linear absorption to occur, the incident electric field strength of the laser must be approximately equal to the ionisation energy of the electron. The excited electrons will transfer the energy to the lattice which causes localised change in the material. This causes localised cracking, void formation, localised melting or localised in refractive index depending on the degree of non-linear absorption (Gattass and Mazur, 2008)

Therefore, mode-locked laser micromachining has a variety of applications in photonics. The various effects of UV radiation on glass has been utilised to fabricate waveguides on glass substrate. The development of mode-locked laser allows for the same fabrication process but with lasers of sub-UV photon energy. Miura et al has demonstrated that waveguides can be fabricated on various types of glass using ultrashort pulse (120 fs) from a Ti:sapphire laser with centre wavelength of 800 nm.
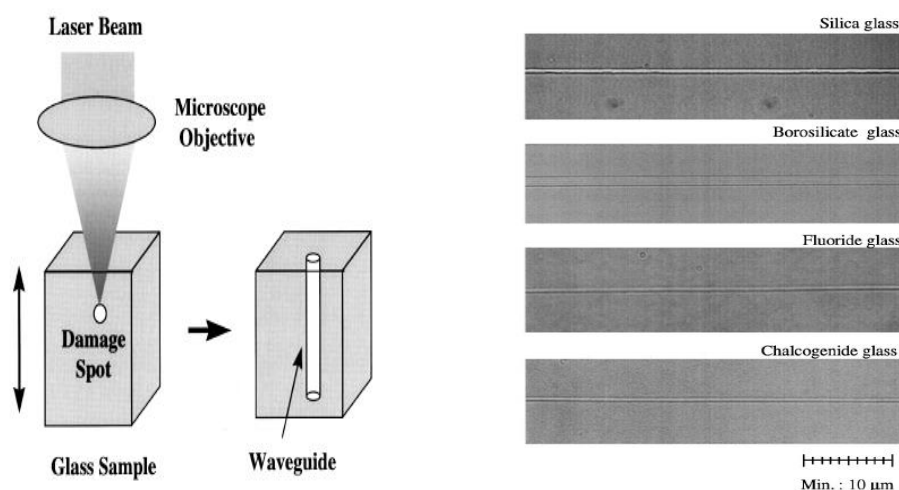
Figure 2.21. Schematic of the waveguide writing process and the result on different types of glass.

Figure 2.21 shows the schematic of the waveguide writing process and the result on different typed of glass. The glass sample is simply translated along the focal point of the objective lens. Visible alteration to the material can be clearly seen on different types of glass. This proves to be a promising method of fabricating waveguides using mode-locked laser (Miura et al., 1997).

In addition to waveguides, the mode-locked laser micromachining has successfully be used to fabricate active devices such as amplifier using Er:Yb-doped phosphate glass. This method has also successfully fabricated electro-optic modulators on lithium niobate substrate. This method has also filters and resonators. The three-dimensional degree of freedom allows for three-dimensional devices to be produced. This method has also proven to be successful in inducing polymerisation using two-photon absorption in resin which opens the avenue for fabrication of polymer waveguide (Gattass and Mazur, 2008).

2.6   Supercontinuum Generation

Nicholson et al (2004) demonstrated supercontinuum using a higly non-linear fibre (HNLF). The fibre is germanium doped silica fibre. Careful design of the incex profile allows for a small effective area, low dipersion and low dispersion slope with low loss. This fibre has non-linear index several times higher than that of standard optical fibres. The fibre has a dispersion of 1.9 ps/(nm km). Furhtermore, the fibre is irradiated to further increase the spectral broadening induced by the fibre. The non-linear index of the fibre is calculated to be 10.6 $W^{-1}km^{-1}$.
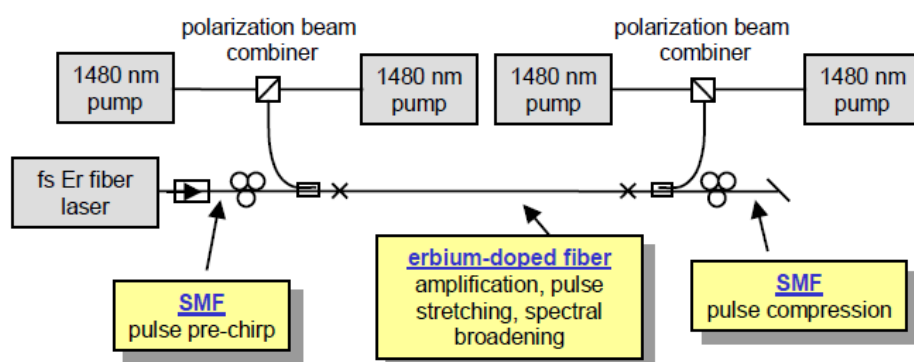
Figure 2.22. Schematic of the laser and amplifier setup (Nicholson et al., 2004).

Figure 2.22 shows the schematic of the laser and amplier setup. The input laser is a mode-locked erbium-doped fibre laser with power of 2 mW, pulse width of 250 fs and repetition rate of 46 MHz. A 2m long EDF is used as the gain medium of the ampilfer. The EDF is pumped biderctionally with peak power in both direction of 610 mW. The single mode fibre at the output of the amplifier is used to compensate the broadening caused by the positive dispersion of the EDF used in the amplifier.
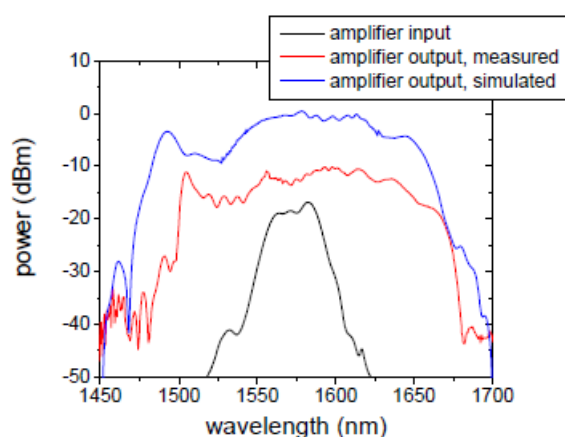
Figure 2.23. Output spectrum of the mode-locekd fibre laser (black), simulated spectrum after the ampliefier (blue) and actual measured sspectrum after the amplifier (red) (Nicholson et al., 2004).

Figure 2.23 shows the output spectrum. The black line shows the spectrum of the mode-locked fibre laser. Due to the positive dispersion of the EDF, the output spectrum is significantly broadened (the SMF is kept as short at possible to minimise compression effects). The peak power of the amplified pules is measured to be 400 mW.

In the experiment, 12 cm of the HNLF is used 8 cm irradiated with UV radiation. The HNLF is directly spliced onto the output of a amplified mode-locked pulses from a fibre laser.
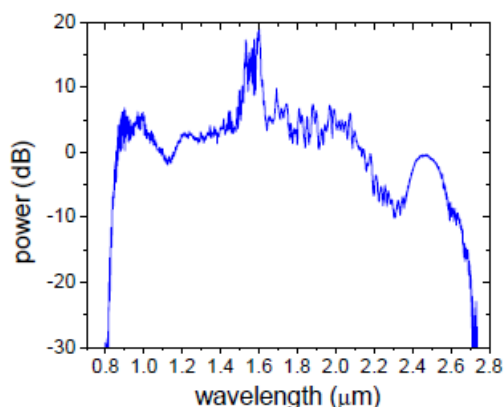
Figure 2.24. Output spectrum of the supercontinuum from the UV exposed
HNLF (Nicholson et al., 2004).

Figure 2.24 shows the supercontimuum observed from the UV exposed
HNLF. The spectral width is approximately 1.65 µm with average power of 400
mW.

2.7   Summary

The mode-locked laser has many applications especially in fabrication of micro-
scale photonic devices such as waveguide, amplifiers, filters and resonators.
Due to the high pulse intensity, the mode-locked laser is useful in many non-
linear optics applications.

Mode-locked fibre laser has been successfully demonstrated using
saturable absorber and with an all-fibre setup. The setup using the saturable
absorber seems to be the most promising as it requires low pump power and is
relatively simple and 2D material shows great potential to be used as a saturable
absorber. Typically, most mode-locked fibre laser power output is limited by
non-linear effects. The output power obtained is only several hundreds of
milliwatts. To achieve output power of exceeding 1 W, the MOPA system is
required. Using a multi-step amplification, the output power can reach up to 100
W.

However, the supercontinnum generation of standard single mode fibre is not well described. It is critical to understand the supercontinuum generation in single mode fibres. Supercontinuum generation will disrupt mode-locked pulses especially after the amplification process. The mode-locked laser is utilised in many researches. Therefore, due to its relatively low cost, the mode-locked fibre laser can be used, and the utility of the mode-locked fibre laser can be further increased with a portable and compact module.

CHAPTER 3

METHODOLOGY AND WORK PLAN

3.1 Introduction

This project involves a few parts. The first part is setting up the laser diode and its connection to the laser current driver and the TEC controller. The laser diode will need to be characterised after the connections are set up The laser cavity will need to be constructed. Once the housing has been built, the laser diode and the optical components will be placed into the housing.

3.2 Laser Safety and Antistatic Precaution

The laser diode that will be used in the fibre laser is the LC96Z600-76 manufactured by II-VI photonics. The laser output has the centre wavelength of 976 nm with spectral width of 2 nm. The maximum output optical power is 600 mW at the maximum drive current of 1 A. This laser diode is rated as a class IV laser.

Extreme precaution must be taken when handling this laser diode not only due to its high power but the output wavelength is outside of the visible range. It is important to avoid exposure of the radiation, either direct or scattered, to the eye and skin (II-VI photonics, 2020).

The laser diode is sensitive to electrostatic discharge. It can be damaged easily from electrostatic discharge (II-VI photonics, 2020). Therefore, it is important to take the necessary precaution to prevent damage to the laser diode. In addition, the laser current driver and the TEC controller can also be damaged by electrostatic discharge. When handling the components, it is important to wear a protective anti-static strap (Hodgson and Olsen, 2020).

3.3 Setting Up the Laser Diode and the Connections to the Laser Current Driver and Thermoelectric Cooler Controller
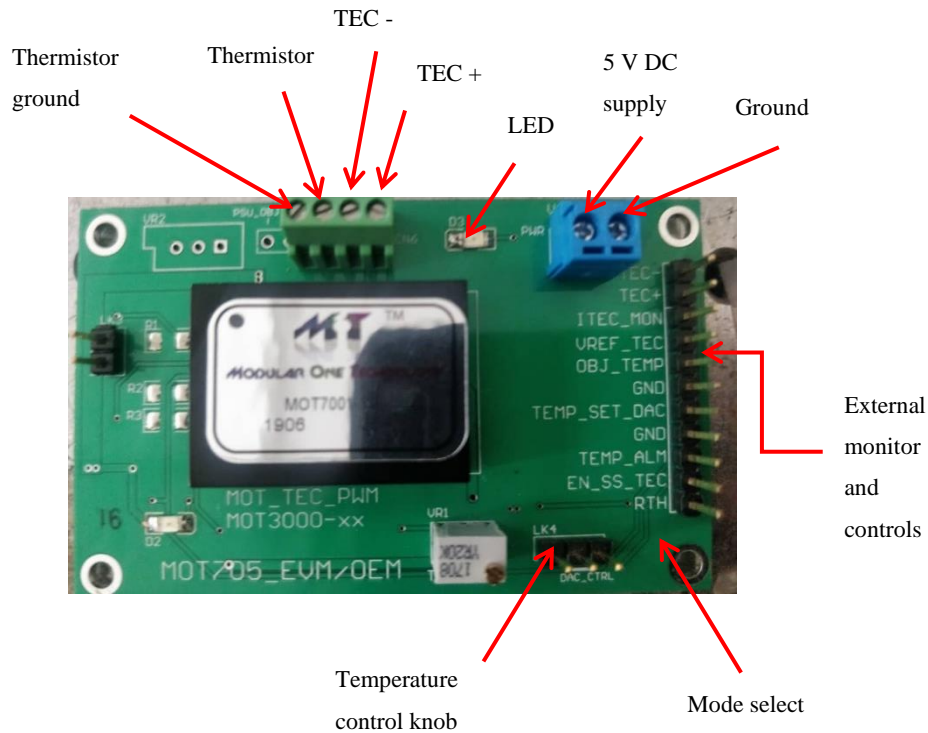
Figure 3.1. TEC controller and the pin configuration.

Figure 3.1 shows the TEC controller (MOT7001-20) on the MOT705_OEM board and the pin configuration on the printed circuit board (PCB). The circuit requires an input of 5 V DC. The TEC controller reads the resistance of the thermistor on the laser diode and controls the current to the TEC to maintain the temperature at a set temperature. To set the temperature to 25°C, the centre pin and the right pin on the mode select will be shorted. This sets the temperature control to external voltage via TEMP_SET_DAC pin on the external monitor and controls. When no voltage is supplied to the pin, internal biasing on the module will automatically set the temperature 25°C. The LED will be illuminated green when the TEC controller is functioning and red when there is an error (Modular One Technology, 2016c).
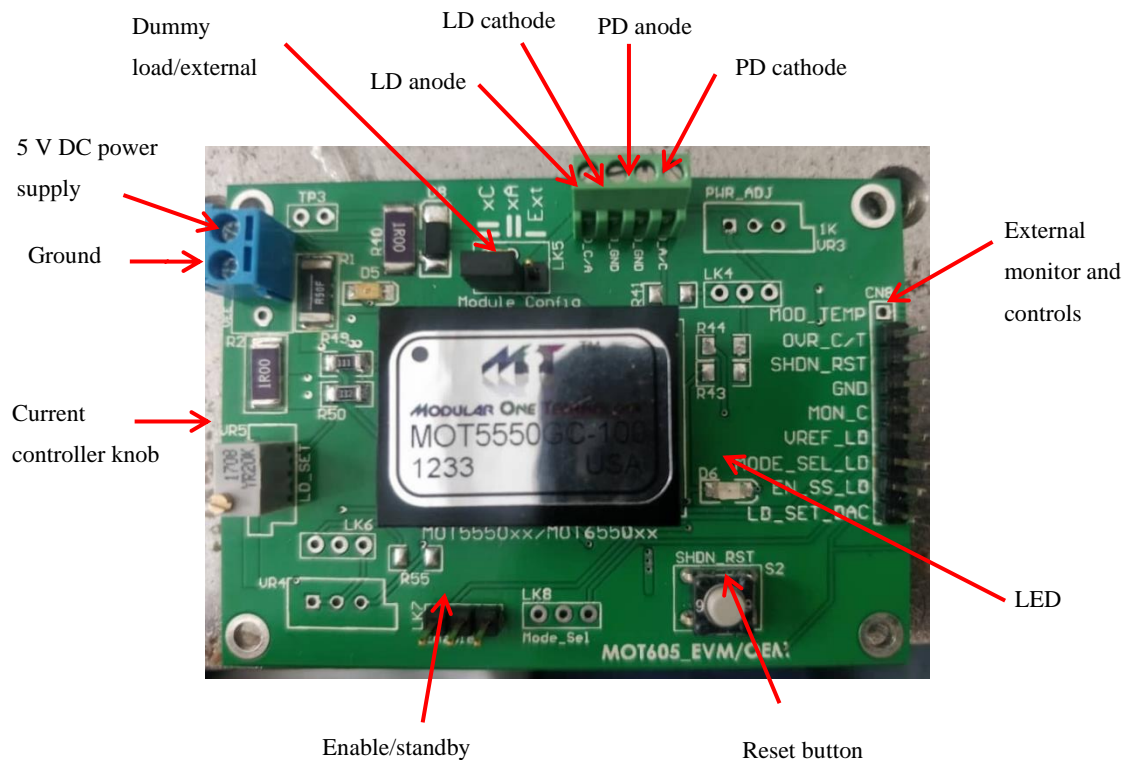
Figure 3.2. Laser current driver and the pin configuration (LD: laser diode, PD: photodiode

Figure 3.2 shows the laser current driver module (MOT5550GC-100) on the MOT605_OEM board. The circuit requires a 5 V DC. No link in the enable/standby pins will set the laser current to be enabled with soft start. Shorting the centre and right pin will set the module to be enabled or disabled via an external voltage at the EN_SS_LD pin at the external monitor and controls. A high voltage will disable the module and a low voltage will enable the module. The current can be controlled using the current control knob. The current can be monitored with the MON_C pin which outputs a voltage from 0 to 2.6 V (Modular One Technology, 2013). The transfer characteristic is 2.6 mV/mA (Modular One Technology, 2016b). The reset button will reset the module when a fault occurs. The board also comes with a dummy load for testing. To connect to the external laser diode, the jumper must be shifted to the external load configuration. The LED will be illuminated green when the laser current driver is functioning and red when there is an error (Modular One Technology, 2013).
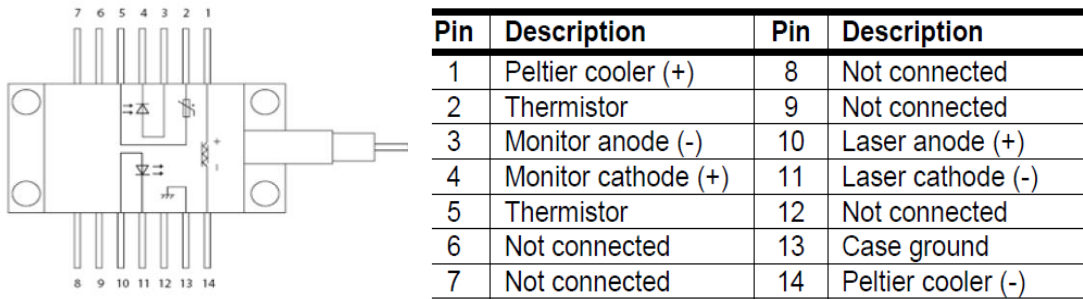
Figure 3.3. Pin configuration of the laser diode (II-VI photonics, 2020).

Pin	Description	Pin	Description
1	Peltier cooler (+)	8	Not connected
2	Thermistor	9	Not connected
3	Monitor anode (-)	10	Laser anode (+)
4	Monitor cathode (+)	11	Laser cathode (-)
5	Thermistor	12	Not connected
6	Not connected	13	Case ground
7	Not connected	14	Peltier cooler (-)
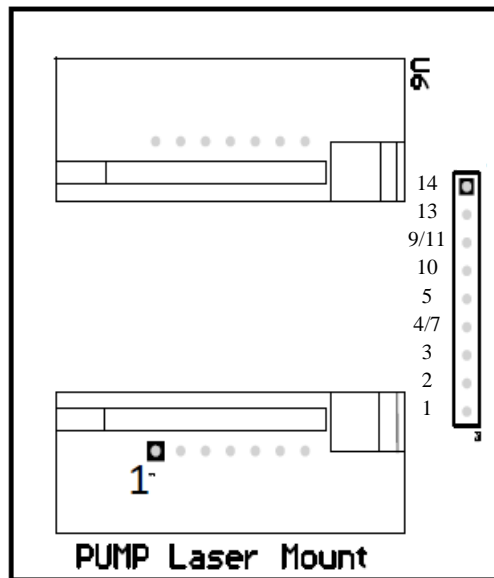
Figure 3.4. Laser diode mount (Modular One Technology, 2016a)

Figure 3.3 shows the pin configuration of the laser diode. The laser diode will be mounted onto a mount as shown in Figure 3.4. The location of pin 1 of the laser diode is indicated in Figure 3.4. The connections to TEC controller and the laser current driver are made through the sockets at the end of the mount.
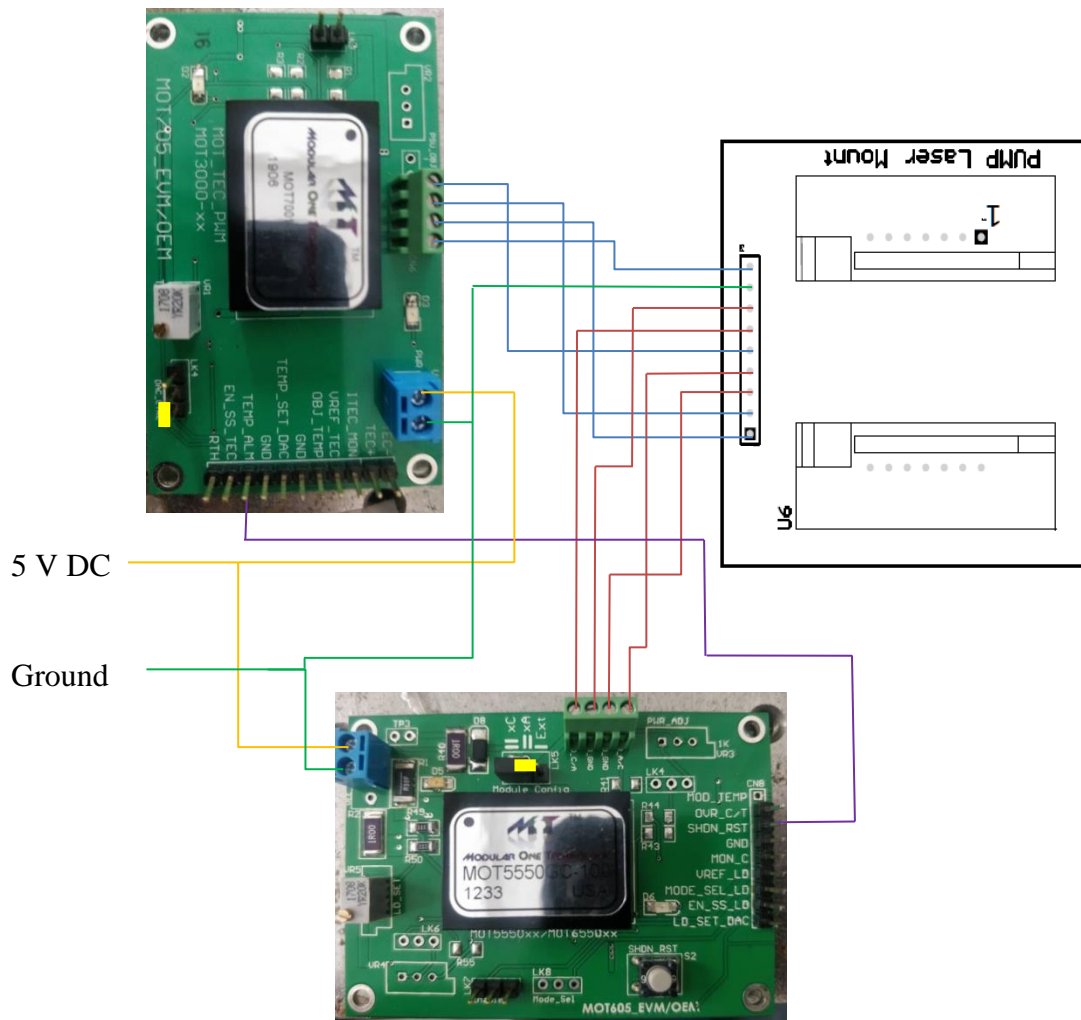
Figure 3.5. Connection between the laser diode mount and the TEC controller and the laser current driver.

Figure 3.5 shows the connection between the laser diode mount and the TEC controller and the laser current driver. The jumper at the load configuration must be shifted to the external position to connect to the eternal laser diode. Since the maximum current drawn by the laser diode and the TEC are 1 A and 2 A respectively, multicore wires are required to make the connections. To supply current to the laser diode, the connection between the EN_SS_LD pin and the power supply will be disconnected. This will protect the laser diode from any current or voltage surges during start up. The voltage TEMP_ALM pin will be low when the temperature falls within $\pm 1.5^{\circ}$C of the temperature set. This pin will be connected to the SHDN_RST pin of the laser current driver. When a low voltage is connected to this pin, the laser current driver will be shut

locking regime utilises the saturable absorber used is tin oxide. The tin oxide film will be sandwiched between two ferules.
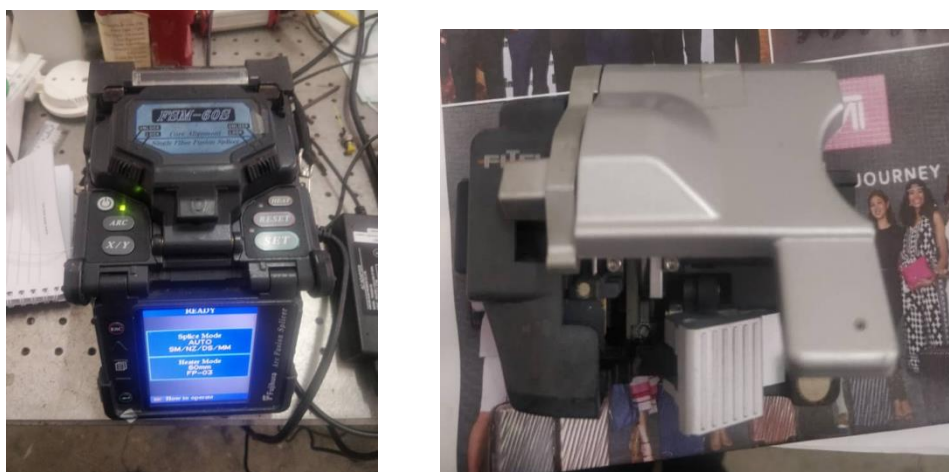
Figure 3.7. The fusion splicer (left) and the optical fibre cleaver (right).

Figure 3.7 shows the fusion splicer and the optical fibre cleaver. Both of these will be used to construct the laser cavity. To build the laser cavity, the single mode fibre and the EDF has to be spliced together. Several optical fibres also need to be spliced to increase the length of the laser cavity. Before the fibres can be spliced together, the jacket and the buffer of the optical fibres has to be stripped off. After stripping off the jacket and buffer, the optical fibres are cleaned with isopropanol. The ends of the optical fibres are cleaved to ensure the ends are flat and perpendicular to the axis of the optical fibre. The optical fibres are placed into the splicer. From the viewing screen, the optical fibres can be inspected. There will be an error is the ends are not cleaved properly. The splicer uses a strong electric field to heat the ends of the optical fibres to melt the ends of the optical fibres so the two fibres can be fused.
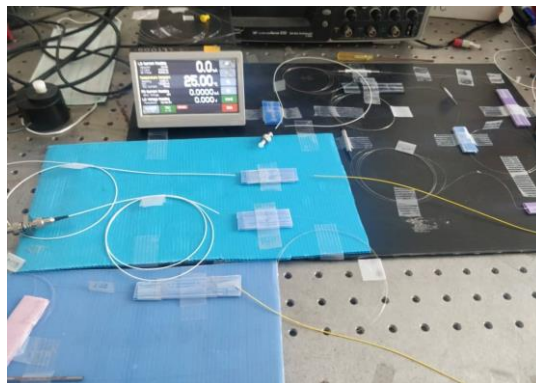
Figure 3.8. Mode-locked fibre laser cavity.

Figure 3.8 shows the mode-locked fibre laser cavity. The gain fibre is pumped with a compact laser diode. This will be replaced with the high-power laser diode when it is placed into the fibre laser module. Only initial testing is done. At the time of writing this report, mode-locked pulses are obtained but the output optical power is low.

3.5 Characterising the Mode-Locked Fibre Laser

After the laser cavity is constructed, the mode-locked fibre laser will be tested. The output of the mode-locked fibre laser is observed using a 5 GHz photodetector (DET08CFC/M InGaAs biased detector) which is connected to a 300 MHz oscilloscope (LeCroy WaveAce 232) with 2 GS/s sampling rate. The bandwidth, pule duration and signal to noise ratio will be measured using an optical spectrum analyser (Yokogawa AQ6370), an autocorrelator (Alnair Labs HAC-200) and RF spectrum analyser (Rohde & Schwarz FPC-100) respectively.

The pump current is increased slowly until the mode-locked pulse train is observed in the oscilloscope. Both fundamental and higher order mode-locking will be obtained. Therefore, both fundamental and higher order mode-locked pulses will be analysed in the same way as previously described.

3.6 Developing and Characterising the Er-doped Fibre Amplifier

To obtain high optical power, the mode-locked fibre laser will be amplified in two stages. The first stage amplification will use a commercial EDFA is the FS 23 dBm single channel in-line EDFA optical amplifier for SDH networks. The second stage amplifier will be developed in the lab.
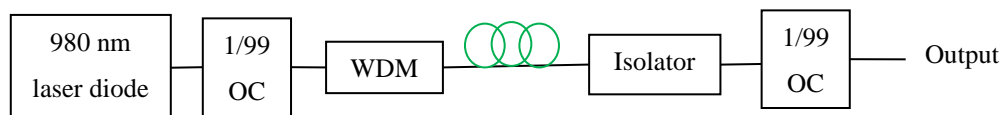
Figure 3.9. Schematic of the EDFA.

Figure 3.9 shows the schematic of the EDFA. The gain medium is 5 m of EDF. The pump laser is the 600 mW 980 nm laser diode. The 1% output from the first 1/99% output coupler is used to monitor the laser diode output. The 980/1500nm WDM is used to input the 1550 nm from the mode-locked fibre laser. The input pulses are amplified by the EDF and the isolator will prevent back reflection into the laser diode and filter out the 980 nm light from the laser diode. The 1% port of the second 1/99% output coupler is used to monitor the amplifier. The output will be amplified 1550 nm mode-locked pulses.

The output power at different pump current will be measured. The output spectrum will be measured with the optical spectrum analyser. In addition, the spectral broadening will be analysed and eliminated if the spectral broadening is at an unacceptable level.

CHAPTER 4

RESULTS AND DISCUSSION

4.1 Introduction

In this section, the results from the chatractrisation of the laser diode will be disucussed followed by the characterisation of the mode-locked fibre laser. The mode-locked pulses will be amplified using a two-step amplification. The amplified mode-locked pulses will be characterised. Non-linear effects causes pulse broadening. The pulse broadening will be described and discussed.

4.2 Laser Diode Characterisation

The laser diode is characterised by measuring the output power at different pump current. The optical power is measured using the S146C optical power meter from Thorlabs. Since the laser diode does not have a fibre pigtail, the fibre end is cleaved and directly inserted into the optical power meter. The laser current driver and TEC controller are both powered on and the laser current is increased and the optical power is measured.
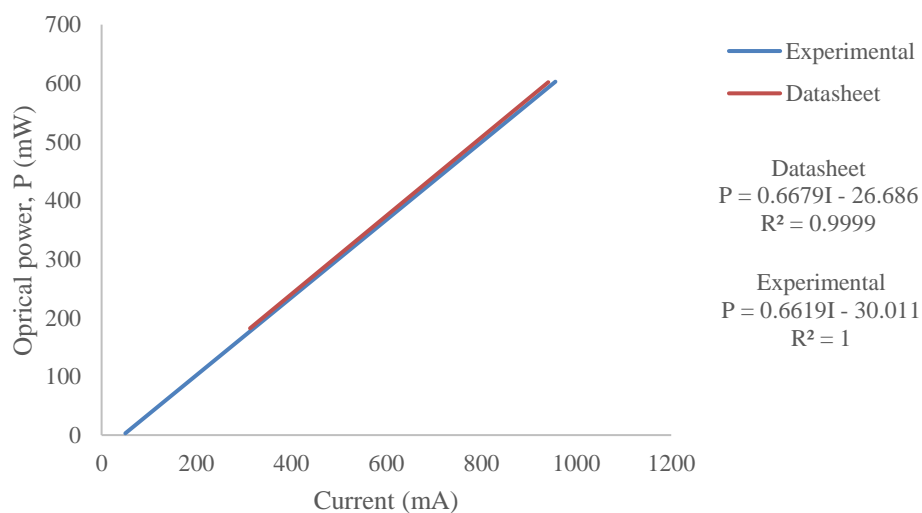
Figure 4.1. Laser diode characterisation.

Figure 4.1 shows the laser diode characteristic. The blue line indicates the experimental result and the red line indicates the data from the datasheet. The R^2 value for the experimental data is 1 which shows that the power increases with current linearly which is the expected behaviour of the laser diode and the slope of the experimental data differs from the datasheet value by 0.601% which indicates that the laser diode is working as expected. The loss could be due to the fibre cleave. The table of data will be attached in Appendix A.

4.3　　　Characterisation of Modde-Locked Pulses
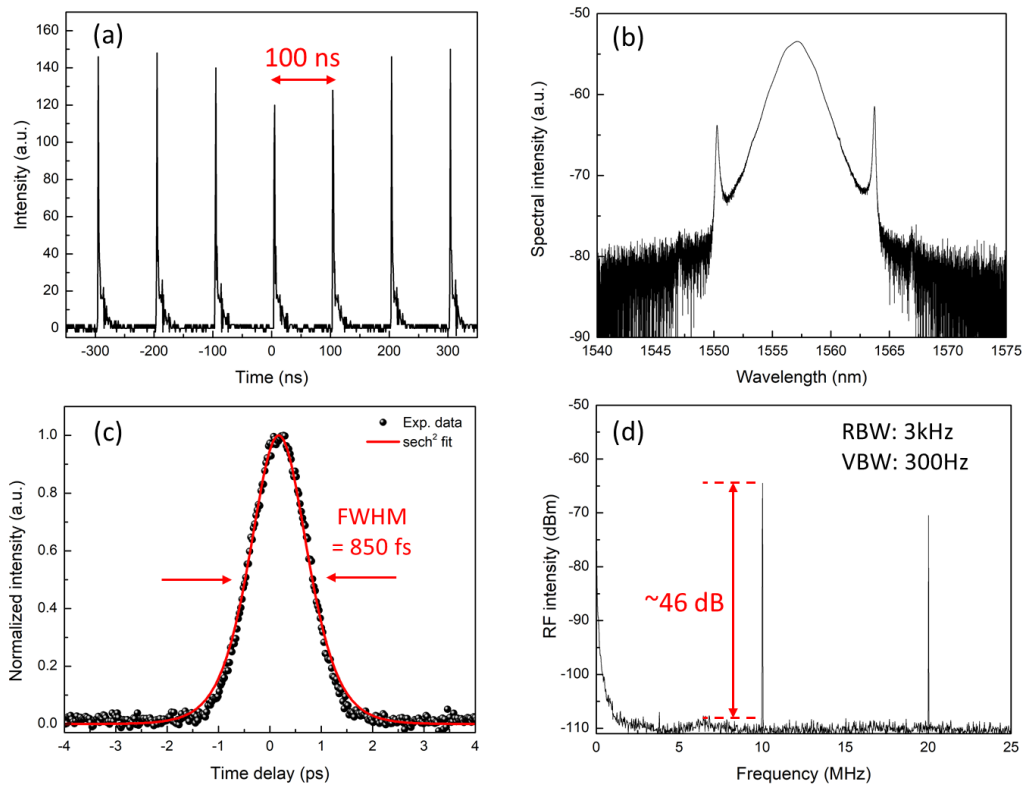
Figure 4.2. Results of the fundamental mode-locking from the mode-locked fibre laser; (a) output pulse train, (b) output spectrum, (c) autocorellator trace and (d) RF spectrum.

When the pump power is increased to 54 mW, continouos wave operation is observed. Once the pump power exceeds 60.4 mW, fundamental mode-locking is observed. Figure 4.2 shows the pulse characteristic of the mode-locked pulses. The repetition rate is 10 MHz with pulse interval of 100 ns. Using simple calculations, assume that the EDF has the same refractive index as the SMF, and using 1.5 for the refractive index of silica, the expected value of the pulse interval for a single pulse propagating in the laser cavity is

$$T = \frac{18.6 + 0.62}{\frac{c}{1.5}}$$

$$= 96.2 \; ns$$

The experimental result agrees well with the expected value for the repetition rate and pulse interval. From the optical spectrum, the 3 dB bandwidth is 3.3091 nm. The central wavelength is 1557 nm with Kelly sidebands. The presence of the Kelly sidebands indicates that the mode-locked pulses are soliton pulses. Soliton pulses are pulses that do not experience temporal or spatial change due to the balance of self-phase modulation from the Kerr effect and chromatic dispersion over the propagation distance. To satisfy the soliton condition, the pulse may shed some of its energy in the form of dispersive waves. These dispersive waves are weaker and do not experience non-linear effects and are broadened due to chromatic dispersion (Paschotta, 2020p). The dispersive waves couples with the soliton pulse to form the Kelly sidebands. As pulse energy is increased (either by decreasing pulse energy or increasing peak power), the Kelly sidebands become more pronounced. The appearance of Kelly sidebands can indicate that the pulse duration is near its minimum (Paschotta, 2020e).

The pulse duration is ~850 fs by using a sech² fit for the autocorrelator trace and measuring the FWHM. The spectral width in frequency domain is

$$\Delta v = \frac{c}{\lambda^2} \Delta \lambda$$

$$= \frac{c}{(1557 \times 10^{-9})^2} (3.3091 \times 10^{-9})$$

$$= 0.409 \times 10^{12} Hz$$

The time bandwidth product is

$$TBP = \Delta v \cdot \Delta t$$
$$= (0.409 \times 10^{12})(850 \times 10^{-15})$$
$$= 0.348$$

A bandwidth-limited (or transform limited) pulse is a pulse with minimum bandwidwidth. For the sech^2 pulse, the minimum time bandwidth product is 0.315 (Paschotta, 2020b). The time bandwidth product of the pulse is higher than the value of the transform limited sech^2 pulse. This indicates that the pulse is chirped but the value is still close to 0.315 which indicates that the pulse width is close to minimum which is consistent with the observation of the Kelly sidebands.

The resolution bandwidth and the video bandwidth of the RF spectrum analyser are 3 kHz and 300 Hz respectively. The SNR is ~46 dB which indicates that the mode-locking regime is stable. The fundamental beat note is 10.02 MHz which confirms the observation from the oscilloscope.

Increasing the pump power will cause higher order mode-locking to be obtained. However, the higher-order mode-locked pulses are non-periodical which is not favourable for optical application. However, this issue is resolved by adjusting the PC. The pump power is increased and then the PC is adjusted while observing the pulse train. The repetition rate indicates the order of the mode-locking. For the nth order mode-locking, the repetition rate is n times the repetition rate of the fundamental mode-locking (10 MHz).
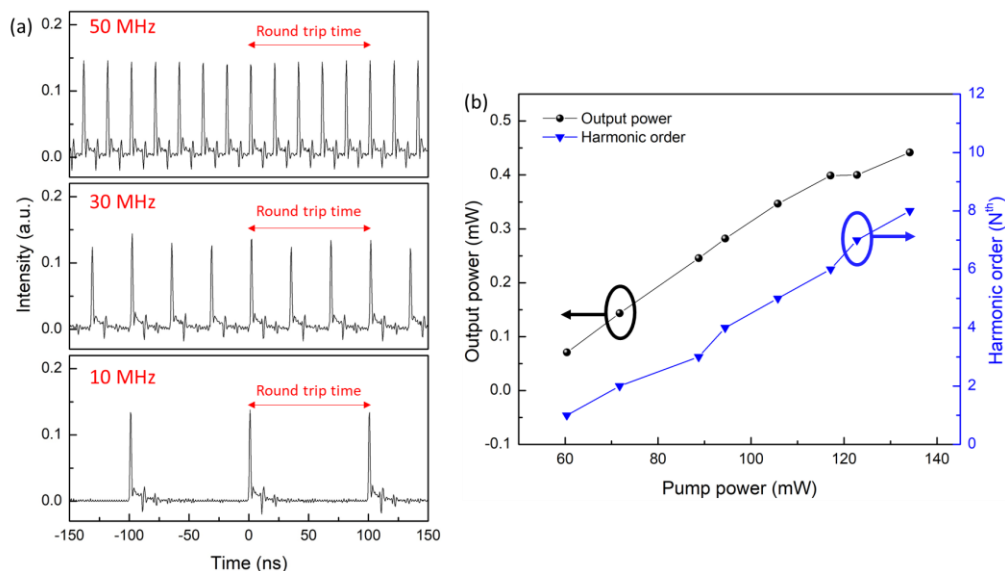
Figure 4.3. Higher order mode-locking. (a) Shows the pulse train of the 5th order (top), 3rd order (middle) and 1st order (bottom) mode-locking. (b) Shows the relationship between the output power and the pump power and the relationship between the harmonic order and the pump power.

Figure 4.3 shows the pulse train of the 1st, 3rd and 5th order mode-locking and relationship between the output power and the pump power and the relationship between the harmonic order and pump power. The harmonic order increase with pump power. The output power also increases with pump power. When the pump power is 134 mW, 8th order mode-locking is obtained. Higher-order mode-locking can be achieved by further increasing the pump power. However, the SNR is below 30 dB. For optical applications, the acceptable SNR for good reliability is 30 dB (Howe, 1987). Therefore, the higher-order mode-locking is not suitable for most optical application and therefore, it is not pursued further.
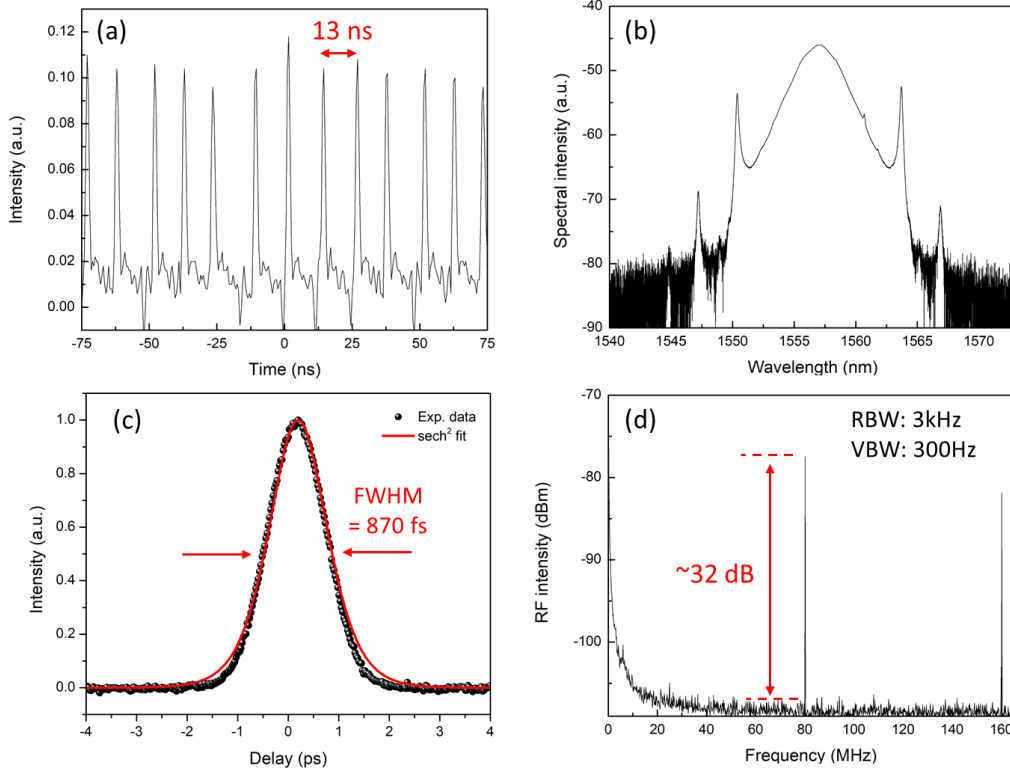
Figure 4.4. 8th order mode-locking. (a) Pulse train, (b) optical spectrum, (c) autocorrelator trace and (d) RF spectrum.

Figure 4.4 shows the results of the 8th order mode-locking. The repetition rate is 77 MHz and the pulse interval is 13 ns. The optical spectrum shows that the central wavelength is 1557 nm and the 3 dB bandwidth is 3.11 nm. The optical spectrum shows that Kelly sidebands are present. This indicates that the pulse width is near the minimum. From the autocorrelator trace and using sech^2 fit, the pulse width is measured to be 870 fs. The time bandwidth product is

$$TBP = \frac{c}{(1557 \times 10^{-9})^2}(3.11 \times 10^{-9}) \times (870 \times 10^{-15})$$

$$= 0.334$$

This indicates that the pulse is chirped and this value together with the appearance of the Kelly sidebands indicates that the pulse width is near the minimum. The SNR is 32 dB with the fundamental beat note at 80.1 MHz. This is in agreement with the pulse train observed from the oscilloscope.

Stability test is carried out for the fundamental and 5th order mode-locking. The test was carried out by turning the laser on continuously for seven

hours and the optical spectrum and optical power is measured and recorded at a twenty-minute interval for the first two hours and at a one-hour interval for the remaining time.
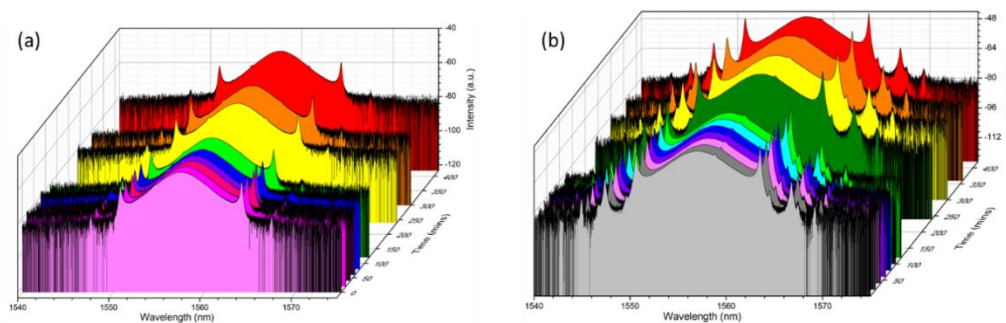
Figure 4.5. Stablity test of the (a) fundamental mode-locking and (b) 5th order mode-locking.

Figure 4.5 shows the stability test of the fundamental and 5th order mode-locking. The optical spectrum does not change over the seven hours operation.
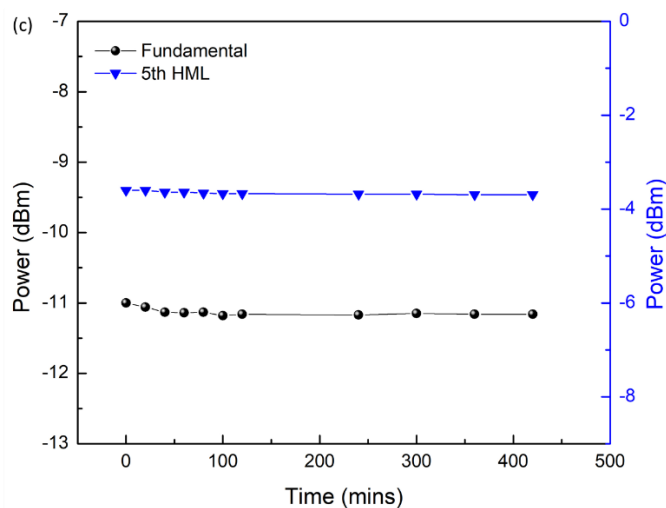
Figure 4.6. Output power measured over seven hours.

Figure 4.6 shows the output power measured over seven hours. The output power varies by ±0.05 dBm and ±0.03 dBm for the fundamental and 5th order mode-locking respectively. The stability test shoes that the GO saturable absorber does not deteriorate over time and is a good candidate for saturable absorber for passively mode-locked fibre laser system.

4.3.1 Development and Characterisation of the EDFA

Figure 3.9 shows the schematic of the of the second EDFA. The components are characterised by measuring the power before and after the component. The current control knob of the laser current driver is turned to increase the current. The current is monitored by the output voltage at the MON_C pin of the laser current driver with the transfer characteristic of 2.6 mV/mA. Each component of the EDFA will be characterised individually.

The first output coupler has a 3.498% loss. The data is shown in Table 4 in Appendix B. Table 5 in Appendix B shows the data from the characterisation of the WDM. The isolator is used to prevent any back reflection from the fibre cleave end to the laser diode which can cause damage to the laser diode. The residual pump and insertion loss of the EDF is shown in Table 6 of Appendix B. The characterisation of the isolator and the second 1/99% output coupler is shown in Table 7 of Appendix B. The isolator and the 1/99% output coupler are characterised together because they are spliced together. The output from the 99% port of the output coupler is used for experiments. The graph of output power against input power is shown in Figure 4.7. The output power from the mode-locekd fibre laser is set to 60 µW. After the first step amplification, the optical power is 53 mW. The R^2 value of the graph is 0.9988 which shows that the output power increases linearly with pump power.
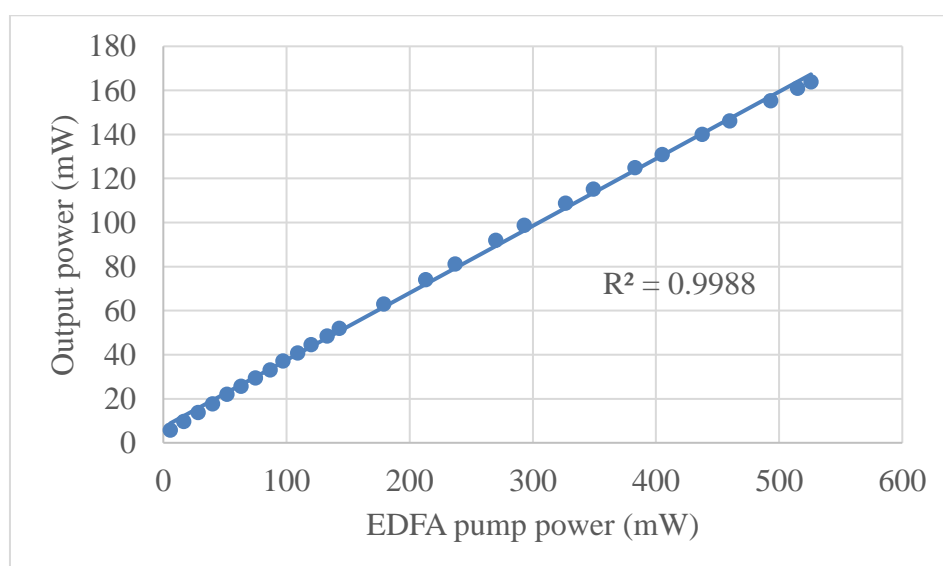
Figure 4.7. Graph of output power against input power.

Table 1. Characterisation of the isolator and second 1/99% output coupler.

MON_C (mV)	980nm LD pump power (mW)	Output power (mW)	
		1%	99%
2522	525.9	13.00	164.00
2470	515.0	12.70	161.00
2366	493.1	12.30	155.30
2210	459.9	11.60	146.20
2106	437.6	11.10	140.10
1950	405.0	10.40	131.00
1846	383.0	9.90	125.00
1690	349.3	9.10	115.30
1586	326.7	8.70	108.80
1430	293.0	7.90	98.80
1326	270.0	7.30	92.00
1170	237.0	6.40	81.20
1066	213.0	5.90	74.10
910	179.0	5.10	63.10
754	143.0	4.20	52.00
702	133.0	3.90	48.50
650	120.0	3.60	44.60
598	109.0	3.30	40.80
546	97.3	3.02	37.20
494	86.8	2.73	33.20
442	74.8	2.42	29.50
390	63.1	2.15	25.70
338	51.7	1.82	22.15
286	40.0	1.52	17.75
234	28.2	1.23	13.9.0
182	16.7	0.95	9.72
130	5.6	0.63	5.90

4.3.2   Pulse Broadenning

The mode-locked pulse is amplified using a commercial EDFA (FS 23 dBm single channel in-line EDFA optical amplifier for SDH networks).
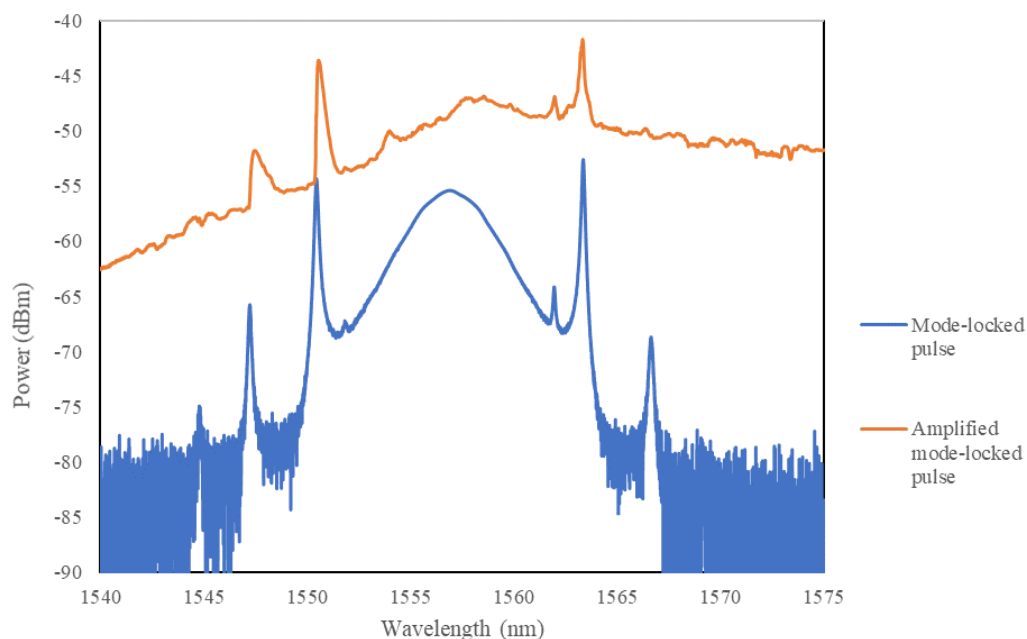
Figure 4.8. The optical spectrum of the mode-locked pulse (blue) and the amplified pulse (orange).

The pump current of the laser diode is set to 180 mA which corresponds to 76 mW. The laser is operating in the second harmonic mode-locking. Figure 4.8 shows the optical spectrum of the mode-locked pulse and amplified mode-locked pulse. The resolution of the optical spectrum analyser is 0.02 nm with sampling rate of one sample every 0.004 nm. The central wavelength is 1557 nm. Before amplification, the average power is -12.3 dBm and after amplification, the average power is 17.25 dBm. The amplified pulse is significantly broadened after amplification. The reason for the pulse broadening is the high intensity of the pulse causing self-phase modulation as the pulse propagates through the optical fibre in the EDFA. Despite the higher peak power, the pulse width is too large. Thus, lowering the intensity which makes the laser not practical for many optical applications. For clarity, the span of the optical spectrum analyser is set to 1500 nm to 1600 nm when analysing the amplified mode-locked pulse as shown Figure 4.9. The pulse no longer has an identifiable

3 dB bandwidth but it can be seen from the spectrum that the pulse stretches from roughly 1550 nm to 1600 nm.
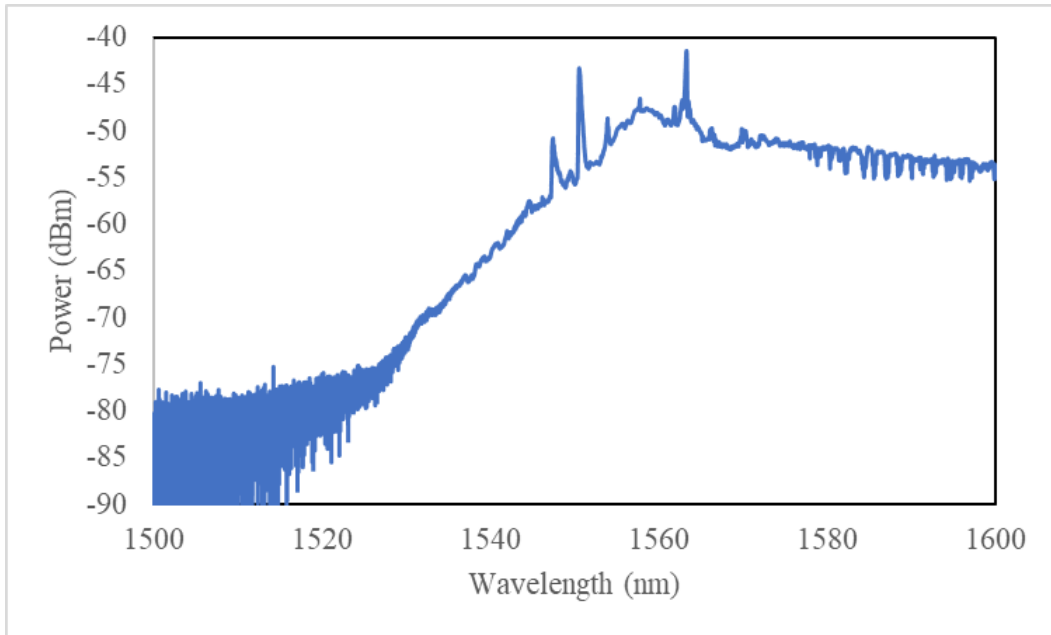
Figure 4.9. Optical spectrum of the amplified mode-locked pulse.

To reduce the intensity of the mode-locked pulses, an additional 2.2 km single mode optical fibre is added before the EDFA to reduce the intensity. The group velocity dispersion of the optical fibre is -22 ps^2/km which corresponds to chromatic dispersion of 414 fs/(km nm). Therefore, the pulse will be broadeneded by

$$\Delta\tau = 414(2.2)(1557)$$
$$= 15071 \, fs$$

The addition of the single mode fibre significantly broadens the pulse and thus, intensity reduces dramatically.
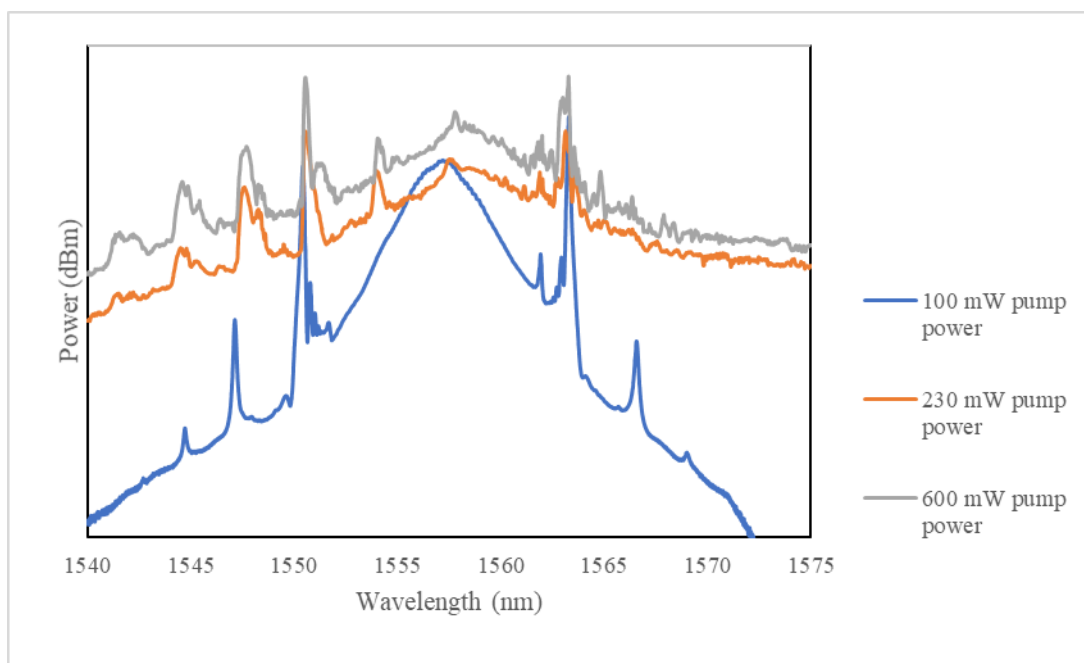
Figure 4.10. Optical spectrum of the mode-locked pulse after the second stage amplification.

Figure 4.10 shows the optical spectrum of the output pulse after the second stage amplification. The pulse width is measured by connecting the 1% port of the 1/99% output coupler to a 20/80% output coupler and connecting the 20% port to a autocorellator. The pulse width when the pump power is 100 mW is ~1 ps. Further increasing the pump power furthers broaden the pulse. Therefore, the optimum pump power for the second stage amplification is 100 mW which corresponds to 192 mA pump current and 0.5 V at the MON_C pin of the laser current driver

The suspected reason for the pulse broadening is the supercontinuum generation. The initial pulse is soliton. In the anomalous dispersion region, the combination of both self-phase modulation and chromatic dispersion causes a complex soliton dynamics where the soliton pulse splits into multiple fundamental soliton pulses which will then couple together to form the broad spectrum.

CHAPTER 5

CONCLUSIONS AND RECOMMENDATIONS

5.1   Conclusions

This research focuses on the focuses on the development of high-power mode-locked fibre laser. The mode-locked fibre laser system is developed using a passive mode-locking with a saturable absorber. The saturable absorber used in this mode-locked fibre laser is GO. The mode-locked fibre laser is able to produce 60 µW (-12.3 dBm) of optical power with the pump power of 76 mW. The pulse width is ~870 fs and the repetition rate is 10 MHz. The SNR is 46 dB which indicates that the mode-locking regime is stable. Stability test over 7 hours shows that the GO saturable absorber does not deteriorate.

To further increase the power, two-stage amplification is done. The first stage is a commercial EDFA with 36 dB gain. The output power after amplification is 53 dBm (17.25 dB). The second amplifier is developed in the lab. After the second stage amplification, the output power can go up to 164 mW (22.1 dBm). The gain of the two-stage amplification can be up to 34.4 dB. This shows that a multi-step amplification process is necessary to obtain a high output power.

Due to the high intensity of the pulse, non-linear effects occur in the fibre. Due to self phase modulation, the pulse is broadenend as it propagates through the amplifier. This process is known as the supercontinuum generation where the femtosecond pulse loses its temporal coherence. This effect is minimised by adding a 2.2 km SMF to broaden the pulse before entering the EDFA to reduce the pulse intensity, thus, reducing the non-linear effects.

5.2   Recommendations for future work

This research has shown that the two stage amplification is able to produce high power mode-locked pulses. The output power can be further increased with more stages of amplification to be comparable with bulk lasers. However, it is necessary to optimise each amplifier individually to reduce pulse broadening due to supercontinuum generation. In addition, the pump for the mode-locked laser can be switched to a high power laser diode.

The mechanism of the supercontinuum generation is too complex for the scope of this research. A detailed simulation of the mechanism of the supercontinuum generation can be done so that the pulse behaviour as it propagates through the fibre can be well described. This is necessary for optimisation of the amplifier. Pulse compression such as prism compressor can be added to the laser system to compress the pulse after the amplification.

The mode-locked fibre laser system can be placed into a module to increase its portability. The casing also helps to protect the optical components and improve the stability of the mode-locking regime by reducing environmental fluctuations on the exposed fibre. The amplifier can also be made into a module to increase its portability. This will help to reduce the bulk of the laser system when multi-stage amplification process is required.

REFERENCES

Ahmed, M.H.M., Latiff, A.A., Arof, H., Ahmad, H. and Harun, S.W., 2016. Optics & Laser Technology Femtosecond mode-locked erbium-doped fi ber laser based on MoS 2 – PVA saturable absorber. *Optics and Laser Technology*, [online] 82, pp.145–149. Available at: <http://dx.doi.org/10.1016/j.optlastec.2016.03.005>.

Chen, S.-P., Chen, H.-W., Hou, J. and Liu, Z.-J., 2009. 100 W all fiber picosecond MOPA laser. *Optics Express*, 17(26), p.24008.

Churin, D., Kieu, K. and Peyghambarian, N., 2012. The role of the saturable absorber in a mode-locked fiber laser. *Fiber Lasers and Applications, FILAS 2012*, 8237, pp.1–6.

Duling, N., 1991. Subpicosecond All-Fibre Erbium Laser. *Electronics Letter*, 27(6), pp.544–545.

Ennejah, T. and Attia, R., 2013. Mode Locked Fiber Lasers, Current Developments in Optical Fiber Technology. In: *Intech*. [online] IntechOpen. Available at: <https://www.intechopen.com/books/current-developments-in-optical-fiber-technology/mode-locked-fiber-lasers>.

FiberLabs Inc, 2020a. *Erbium-Doped Fiber Amplifier (EDFA)*. [online] Available at: <https://www.fiberlabs.com/glossary/erbium-doped-fiber-amplifier/> [Accessed 18 Apr. 2020].

FiberLabs Inc, 2020b. *Fiber laser*. [online] Available at: <https://www.fiberlabs.com/glossary/fiber-laser/> [Accessed 23 Mar. 2020].

Gattass, R.R. and Mazur, E., 2008. Femtosecond laser micromachining in transparent materials. *Nature Photonics*, 2(2008), pp.219–225.

Hecht, J., 2010. *Short history of laser development*. [online] Available at: <https://www.spiedigitallibrary.org/journals/optical-engineering/volume-49/issue-9/091002/Short-history-of-laser-development/10.1117/1.3483597.full?SSO=1> [Accessed 16 Mar. 2020].

Hodgson, D. and Olsen, B., 2020. *Protecting Your Laser Diode*. [online] Available at: <https://www.newport.com/medias/sys_master/images/images/hc0/h01/87970 49454622/AN03-Protecting-Your-Laser-Diode.pdf> [Accessed 22 Mar. 2020].

Howe, D.G., 1987. Signal-To-Noise Ratio (SNR) For Reliable Data Recording. In: R.P. Freese, A.A. Jamberdino and M.R. de Haan, eds. *Optical Mass Data*

Storage II. [online] SPIE.pp.255–261. Available at: <https://doi.org/10.1117/12.936846>.

II-VI photonics, 2020. *LC96Z***-7*.* [online] Available at: <https://www.ii-vi-photonics.com/products/data/D50561-PB.pdf> [Accessed 23 Mar. 2020].

Krylov, A.A., Chernysheva, M.A., Chernykh, D.S. and Tupitsyn, I.M., 2013. A high power MOPA-laser based on a mode-locked thulium-doped fiber oscillator with intracavity dispersion management. *Laser Physics*, 23(4).

laserfocusworld, 2020. *FIBER LASERS: Fiber lasers: The state of the art.* [online] Available at: <https://www.laserfocusworld.com/test-measurement/spectroscopy/article/16549567/fiber-lasers-fiber-lasers-the-state-of-the-art> [Accessed 16 Mar. 2020].

Li, L., Su, Y., Wang, Y., Wang, X., Wang, Y., Li, X., Mao, D. and Si, J., 2016. Femtosecond passively Er-doped mode-locked fiber laser with WS 2 solution saturable absorber. *IEEE Journal of Selected Topics in Quantum Electronics*, 23(1), pp.1–7.

Liu, X., Wang, H., Yan, Z., Wang, Y., Zhao, W., Zhang, L., Yang, Z., Hu, X., Li, X., Shen, D. and Chen, G., 2012. passively mode-locked laser based on a 45 ° -tilted fiber grating. *Optics Express*, 20(17), pp.19000–19005.

Miura, K., Qiu, J., Inouye, H., Mitsuyu, T. and Hirao, K., 1997. Photowritten optical waveguides in various glasses with ultrashort pulse laser. *Applied Physics Letters*, 71(23), pp.3329–3331.

Modular One Technology, 2013. *MOT605_OEM Users Guide.* [online] Available at: <https://www.modularonetechnology.com/Laser-Driver-Boards.htm> [Accessed 23 Mar. 2020].

Modular One Technology, 2016a. *ModularOne Technology Laser Mounts.* [online] Available at: <https://www.modularonetechnology.com/Laser-MOunt-Products.htm> [Accessed 23 Mar. 2020].

Modular One Technology, 2016b. *MOT5550GC & MOT5550GA Series.* [online] Available at: <https://www.modularonetechnology.com/Constant-Current-Drivers.htm> [Accessed 23 Mar. 2020].

Modular One Technology, 2016c. *MOT705_OEM Users Guide.* [online] Available at: <https://www.modularonetechnology.com/TEC-Controller-Boards.htm> [Accessed 23 Mar. 2020].

Nicholson, J.W., Yablon, A.D., Westbrook, P.S., Feder, K.S. and Yan, M.F., 2004. High power, single mode, all-fiber source of femtosecond pulses at 1550

nm and its use in supercontinuum generation. *Optics Express*, 12(13), p.3025.

Paschotta, R., 2020a. *Amplifier Chains*. [online] RP Photonics. Available at: <https://www.rp-photonics.com/amplifier_chains.html> [Accessed 18 Apr. 2020].

Paschotta, R., 2020b. *Bandwidth-limited Pulses*. [online] RP Photonics. Available at: <https://www.rp-photonics.com/bandwidth_limited_pulses.html> [Accessed 2 Aug. 2020].

Paschotta, R., 2020c. *Fiber Amplifiers*. [online] RP Photonics. Available at: <https://www.rp-photonics.com/fiber_amplifiers.html> [Accessed 18 Apr. 2020].

Paschotta, R., 2020d. *Fiber Lasers*. [online] RP Photonics. Available at: <https://www.rp-photonics.com/fiber_lasers.html> [Accessed 16 Mar. 2020].

Paschotta, R., 2020e. *Kelly Sidebands*. [online] RP Photonics. Available at: <https://www.rp-photonics.com/kelly_sidebands.html> [Accessed 2 Aug. 2020].

Paschotta, R., 2020f. *Kerr Effect*. [online] RP Photonics. Available at: <https://www.rp-photonics.com/kerr_effect.html> [Accessed 15 Jul. 2020].

Paschotta, R., 2020g. *Kerr Effect*. [online] RP Photonics. Available at: <https://www.rp-photonics.com/kerr_effect.html> [Accessed 23 Mar. 2020].

Paschotta, R., 2020h. *Master Oscillator Fiber Amplifier*. [online] RP Photonics. Available at: <https://www.rp-photonics.com/master_oscillator_fiber_amplifier.html> [Accessed 13 Mar. 2020].

Paschotta, R., 2020i. *Master Oscillator Power Amplifier*. [online] RP Photonics. Available at: <https://www.rp-photonics.com/master_oscillator_power_amplifier.html> [Accessed 23 Mar. 2020].

Paschotta, R., 2020j. *Mode-locked Fiber Lasers*. [online] RP Photonics. Available at: <https://www.rp-photonics.com/mode_locked_fiber_lasers.html> [Accessed 16 Mar. 2020].

Paschotta, R., 2020k. *Mode-locked Lasers*. [online] RP Photonics. Available at: <https://www.rp-photonics.com/mode_locked_lasers.html> [Accessed 23 Mar. 2020].

Paschotta, R., 2020l. *Mode Locking*. [online] RP Photonics. Available at:

<https://www.rp-photonics.com/mode_locking.html> [Accessed 16 Mar. 2020].

Paschotta, R., 2020m. *Saturable Absorbers*. [online] RP Photonics. Available at: <https://www.rp-photonics.com/saturable_absorbers.html> [Accessed 23 Mar. 2020].

Paschotta, R., 2020n. *Saturation Power*. [online] RP Photonics. Available at: <https://www.rp-photonics.com/saturation_power.html> [Accessed 18 Apr. 2020].

Paschotta, R., 2020o. *Self-phase Modulation*. [online] RP Photonics. Available at: <https://www.rp-photonics.com/self_phase_modulation.html> [Accessed 15 Jul. 2020].

Paschotta, R., 2020p. *Solitons*. [online] RP Photonics. Available at: <https://www.rp-photonics.com/solitons.html> [Accessed 2 Aug. 2020].

Paschotta, R., 2020q. *Supercontinuum Generation*. [online] RP Photonics. Available at: <https://www.rp-photonics.com/supercontinuum_generation.html> [Accessed 15 Jul. 2020].

Paschotta, R., 2020r. *Z-scan Measurements*. [online] RP Photonics. Available at: <https://www.rp-photonics.com/z_scan_measurements.html> [Accessed 19 Mar. 2020].

APPENDICES

Appendix A: Characterisation of the 980 nm 600 W Laser Diode

Table 2. Experimental data.

MON_C (mV)	Current (mA)	Power (mW)	MON_C (mV)	Current (mA)	Power (mW)
2485.6	956	600.0	1274	490	295.0
2470	950	597.5	1222	470	283.0
2418	930	586.7	1170	450	270.0
2366	910	571.0	1118	430	257.0
2314	890	559.4	1066	410	243.0
2262	870	545.0	1014	390	230.0
2210	850	532.5	962	370	215.0
2158	830	518.0	910	350	202.0
2106	810	506.0	858	330	189.0
2054	790	493.0	806	310	175.0
2002	770	478.0	754	290	161.0
1950	750	466.0	702	270	148.0
1898	730	453.0	650	250	135.0
1846	710	440.0	598	230	120.0
1794	690	426.0	546	210	107.0
1742	670	414.0	494	190	94.0
1690	650	401.0	442	170	81.0
1638	630	388.0	390	150	69.0
1586	610	375.5	338	130	55.4.0
1534	590	361.7	286	110	43.0
1482	570	347.0	234	90	28.0
1430	550	334.0	182	70	15.7
1378	530	322.0	130	50	4.40
1326	510	309.0			

Table 3. Data from the datasheet.

Current (mA)	Power (mW)	Current (mA)	Power (mW)
312.7	180	638.9	400
327.7	190	653.3	410
341.3	200	667.8	420
355.4	210	683.0	430
369.2	220	697.3	440
384.3	230	712.3	450
398.9	240	726.2	460
413.5	250	741.3	470
429.2	260	757.4	480
443.9	270	771.8	490
458.2	280	788.5	500
473.6	290	802.9	510
488.7	300	818.4	520
503.3	310	834.6	530
518.3	320	849.3	540
533.7	330	864.3	550
548.1	340	879.8	560
563.6	350	894.1	570
579.1	360	910.4	580
594.0	370	925.5	590
608.2	380	941.0	600
623.9	390		

Appendix B: Characterisation of the EDFA

Characterisation of the 1/99% Output Coupler

Table 4. Characterisation of loss of the 1/99% output coupler.

MON_C (mV)	Current (mA)	Power (mW)			Check (%)		Loss (%)
		Before 1/99	1% port	99% port	1% port	99% port	
2574	990	580	7.28	556	1.255172	95.86207	4.137931
2548	980	573	7.22	551	1.260035	96.16056	3.839442
2522	970	567	7.14	546	1.259259	96.2963	3.703704
2496	960	562	7.07	540	1.258007	96.08541	3.914591
2485.6	956	561	7.04	538	1.254902	95.90018	4.099822
2470	950	556	7	535	1.258993	96.22302	3.776978
2418	930	545	6.86	524	1.258716	96.14679	3.853211
2366	910	533	6.71	513	1.258912	96.24765	3.752345
2314	890	521	6.56	501	1.259117	96.16123	3.838772
2262	870	509	6.4	490	1.257367	96.26719	3.732809
2210	850	497	6.24	478	1.255533	96.17706	3.822938
2158	830	485	6.09	467	1.25567	96.28866	3.71134
2106	810	472	5.94	455	1.258475	96.39831	3.601695
2054	790	462	5.79	444	1.253247	96.1039	3.896104
2002	770	450	5.63	432	1.251111	96.0000	4.000000
1950	750	439	5.48	421	1.248292	95.89977	4.100228
1898	730	427	5.33	410	1.248244	96.01874	3.981265
1846	710	415	5.17	398	1.245783	95.90361	4.096386
1794	690	403	5.04	387	1.25062	96.02978	3.970223
1742	670	391	4.88	375	1.248082	95.90793	4.092072
1690	650	379	4.73	363	1.248021	95.77836	4.221636
1638	630	367	4.57	352	1.245232	95.91281	4.087193
1586	610	355	4.42	340	1.24507	95.77465	4.225352
1534	590	342	4.26	328	1.245614	95.90643	4.093567
1482	570	330	4.11	316	1.245455	95.75758	4.242424
1430	550	319	3.96	305	1.241379	95.61129	4.388715
1378	530	302	3.81	293	1.261589	97.01987	2.980132
1326	510	290	3.66	281	1.262069	96.89655	3.103448

MON_C (mV)	Current (mA)	Power (mW)			Check (%)		Loss (%)
		Before 1/99	1% port	99% port	1% port	99% port	
1274	490	279.0	3.500	270.0	1.25448	96.77419	3.225806
1222	470	267.0	3.350	258.0	1.254682	96.62921	3.370787
1170	450	254.0	3.190	246.0	1.255906	96.85039	3.149606
1118	430	241.9	3.030	234.0	1.257261	97.09544	2.904564
1066	410	229.0	2.880	222.0	1.257642	96.94323	3.056769
1014	390	219.0	2.720	211.0	1.242009	96.34703	3.652968
962	370	205.0	2.570	199.0	1.253659	97.07317	2.926829
910	350	193.0	2.400	187.0	1.243523	96.89119	3.108808
858	330	180.0	2.250	174.0	1.250000	96.66667	3.333333
806	310	168.0	2.120	162.0	1.261905	96.42857	3.571429
754	290	156.0	1.940	150.0	1.24359	96.15385	3.846154
702	270	143.0	1.770	137.0	1.237762	95.8042	4.195804
650	250	130.0	1.620	125.0	1.246154	96.15385	3.846154
598	230	116.0	1.460	113.0	1.258621	97.41379	2.586207
546	210	103.0	1.300	101.0	1.262136	98.05825	1.941748
494	190	91.5	1.140	89.0	1.245902	97.26776	2.73224
442	170	79.0	0.990	77.0	1.253165	97.46835	2.531646
390	150	67.0	0.844	66.0	1.259701	98.50746	1.492537
338	130	55.4	0.690	54.3	1.245487	98.01444	1.98556
286	110	42.0	0.528	41.5	1.257143	98.80952	1.190476
234	90	30.0	0.382	29.7	1.273333	99.00000	1.000000
182	70	18.8	0.236	18.5	1.255319	98.40426	1.595745
130	50	7.6	0.093	7.0	1.223684	92.10526	7.894737
Average					1.252608	96.50188	3.498122

Table 5. Characterisation of loss of the 980/1550 nm WDM.

MON_C (mV)	Current (mA)	Input (mW)	After WDM (mW)	Loss (%)
2548	980	551	530.8	0.162207
2522	970	546	525.9	0.162895
2496	960	540	520.7	0.158062
2485.6	956	538	518.2	0.162849
2470	950	535	515.0	0.165466
2418	930	524	504.1	0.168146
2366	910	513	493.1	0.171824
2314	890	501	482.2	0.166105
2262	870	490	470.8	0.173596
2210	850	478	459.9	0.167645
2158	830	467	449.0	0.170705
2106	810	455	437.6	0.169341
2054	790	444	426.6	0.173621
2002	770	432	415.8	0.165993
1950	750	421	405.0	0.168271
1898	730	410	393.8	0.175081
1846	710	398	383.0	0.166843
1794	690	387	371.8	0.174016
1742	670	375	360.8	0.167647
1690	650	363	349.3	0.167080
1638	630	352	338.2	0.173691
1586	610	340	326.7	0.173298
1534	590	328	315.8	0.164617
1482	570	316	304.0	0.168135
1430	550	305	293.0	0.174322
1378	530	293	282.0	0.166185
1326	510	281	270.0	0.173426
1274	490	270	259.0	0.180640
1222	470	258	248.0	0.171680
1170	450	246	237.0	0.161868
1118	430	234	225.0	0.170333
1066	410	222	213.0	0.179734
1014	390	211	202.0	0.189311
962	370	199	191.0	0.178197
910	350	187	179.0	0.189886
858	330	174	166.0	0.204412
806	310	162	155.0	0.191833

MON_C (mV)	Current (mA)	Input (mW)	After WDM (mW)	Loss (%)
754	290	150	143.0	0.20755
702	270	137	133.0	0.12869
650	250	125	120.0	0.17729
598	230	113	109.0	0.15652
546	210	101	97.3.0	0.16209
494	190	89	86.8	0.10870
442	170	77	74.8	0.12589
390	150	66	63.1	0.19515
338	130	54.3	51.7	0.21309
286	110	41.5	40.0	0.15988
234	90	29.7	28.2	0.22507
182	70	18.5	16.7	0.44455
130	50	7	5.6	0.96910

Table 6. Characterisation of the EDF.

Current (mA)	Input (mW)	Output power (mW)		EDF loss (dB)
		With EDF	Without EDF	
950	517.206	47.500	376.8	8.994172845
900	488.921	45.000	357.00	8.994557023
850	460.636	42.000	336.70	9.03993826
800	432.351	39.000	317.00	9.099946552
750	404.066	37.000	297.00	9.045547253
700	375.781	34.000	277.40	9.116275397
650	347.496	31.000	257.00	9.185714295
600	319.211	28.000	236.50	9.266731137
550	290.926	25.500	216.50	9.289177203
500	262.641	22.800	196.00	9.343212244
450	234.356	20.050	175.20	9.414197249
400	206.071	17.250	154.50	9.521393844
350	177.786	14.550	133.60	9.629434648
300	149.501	11.900	112.00	9.736710613
250	121.216	9.330	89.00	9.795083629
230	109.902	8.300	81.50	9.920795164
210	98.588	7.280	73.00	10.01191481
190	87.274	6.280	64.70	10.12944637
170	75.96	5.320	56.05	10.22663985
150	64.646	4.380	47.70	10.37044269
130	53.332	3.440	39.45	10.59488565
110	42.018	2.550	29.10	10.57352809
90	30.704	1.640	20.90	11.05302438
70	19.390	0.770	12.50	12.10419288
50	8.076	0.009	4.35	26.84246748

Table 7. Characterisation of the isolator and second 1/99% output coupler.

MON_C (mV)	Current (mA)	Input (mW)	After isolator (mW)	After 2nd coupler (mW)	
				1% (µW)	99% (mW)
2522	970	525.9	42.5000	2360.0	32.5000
2470	950	515.0	42.0000	2370.0	32.0000
2366	910	493.1	41.4000	2330.0	31.2000
2210	850	459.9	40.0000	2240.0	30.3000
2106	810	437.6	39.2000	2190.0	29.5000
1950	750	405.0	37.7000	2090.0	28.5000
1846	710	383.0	36.4000	2020.0	27.3000
1690	650	349.3	34.4000	1900.0	25.7000
1586	610	326.7	32.8000	1815.0	24.5000
1430	550	293.0	30.2000	1660.0	22.5000
1326	510	270.0	28.4000	1560.0	21.1000
1170	450	237.0	25.2000	1390.0	18.6000
1066	410	213.0	23.1000	1270.0	17.2000
910	350	179.0	19.6000	1080.0	14.6000
754	290	143.0	15.9000	888.0	11.9500
702	270	133.0	14.7000	815.0	11.0000
650	250	120.0	13.3000	745.0	10.1000
598	230	109.0	12.0000	673.0	9.0500
546	210	97.3	10.6000	598.0	8.0500
494	190	86.8	9.2700	526.0	7.1000
442	170	74.8	7.9000	451.0	6.0400
390	150	63.1	6.4200	376.0	4.9900
338	130	51.7	4.9600	295.5	4.0000
286	110	40.0	3.4400	186.0	2.5000
234	90	28.2	1.9900	108.5	1.4700
182	70	16.7	0.6500	32.4	0.4400
130	50	5.6	0.0024	-	0.0018